

Status, Experimental Results and Perspectives of the ALICE experiment.

Valeria Muccifora

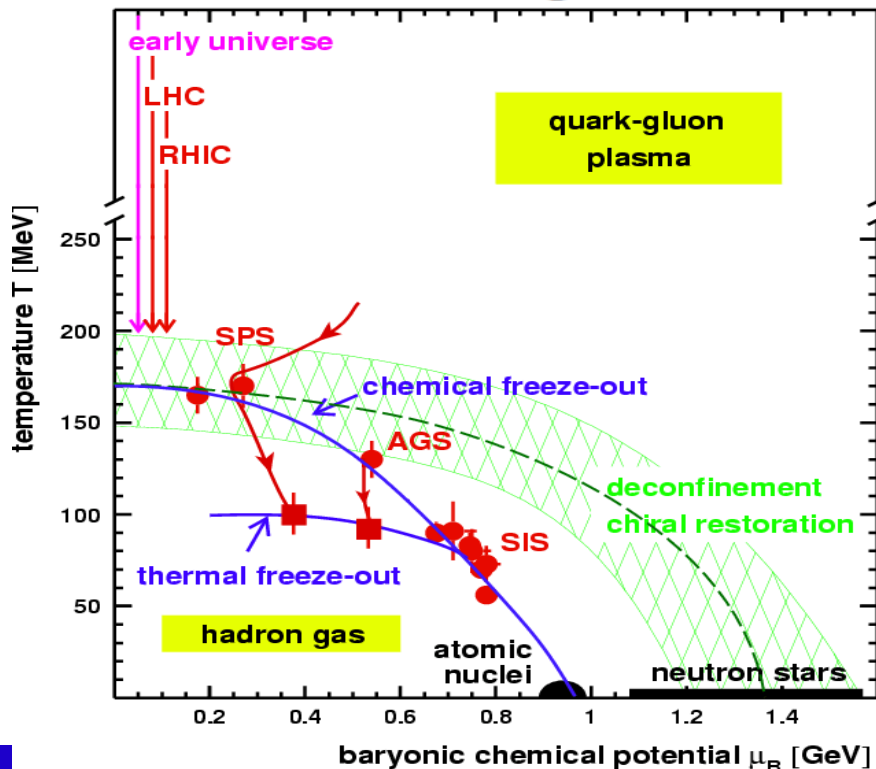


- Status of the LHC heavy ion program
- Recent results
- Perspectives and upgrades

Quark Gluon Plasma

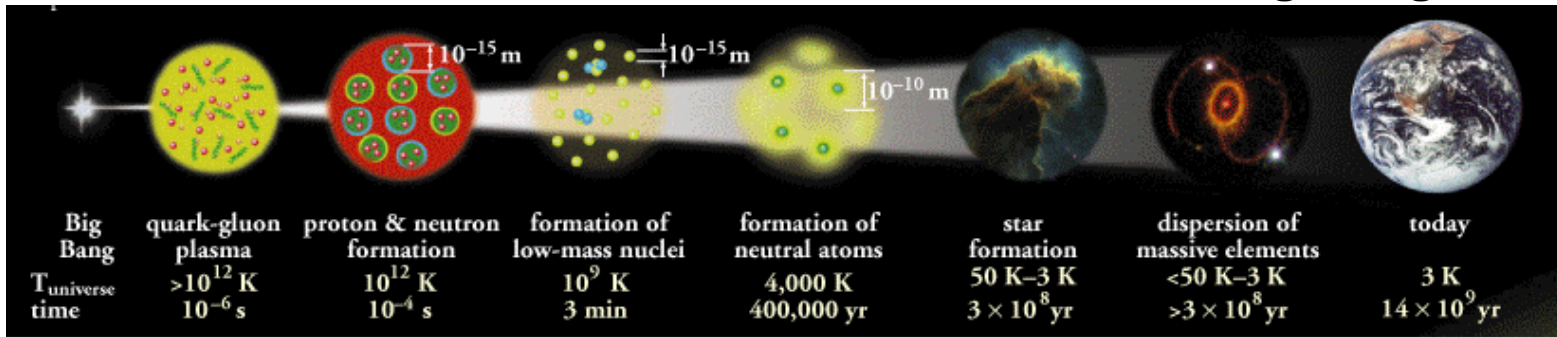
- ◆ Explore the deconfined phase of QCD matter
- ◆ **High-energy nucleus-nucleus** → **large energy density**
($\sim 15 \text{ GeV}/\text{fm}^3$ at LHC) over a **large volume** ($\sim 5000 \text{ fm}^3$ at LHC)

QCD Phase Diagram



Quark Gluon Plasma and Heavy ions

- ➔ Quark Gluon Plasma is a state of strongly interacting matter in which quarks and gluons are no more confined into hadrons
- ➔ QGP is formed at high temperatures and/or density → conditions similar to those achieved few micro-seconds after the Big-Bang

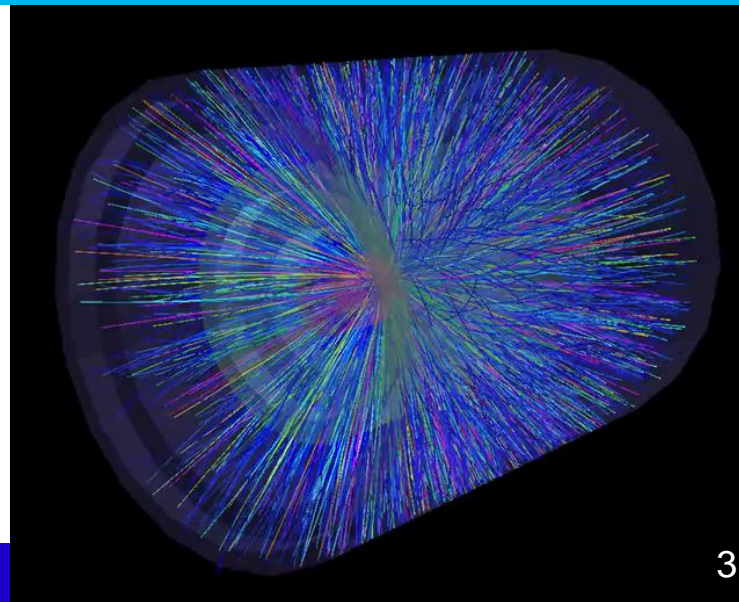


➔ How can QGP be produced in laboratory?

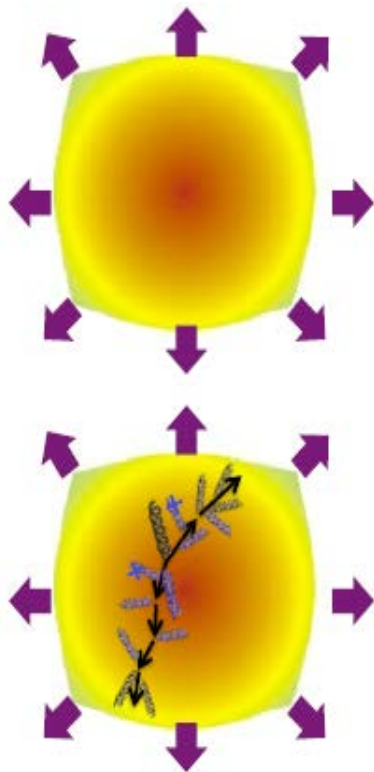
heavy-ion collisions

➔ How to understand the properties of the created hot medium?

study specific probes as jets, open heavy flavors, quarkonium...



The exploration of the QGP: soft and hard probes



“Soft” probes

(e.g. light-flavour particle spectra and flow at low p_T)

Probe system as a whole

Test hydrodynamic description to extract global properties of the medium and of its evolution (e.g. temperature, density, homogeneity, viscosity, expansion velocity)

“Hard” probes

(e.g. high p_T particles, heavy flavours, quarkonia, jets)

Access microscopic processes in the medium

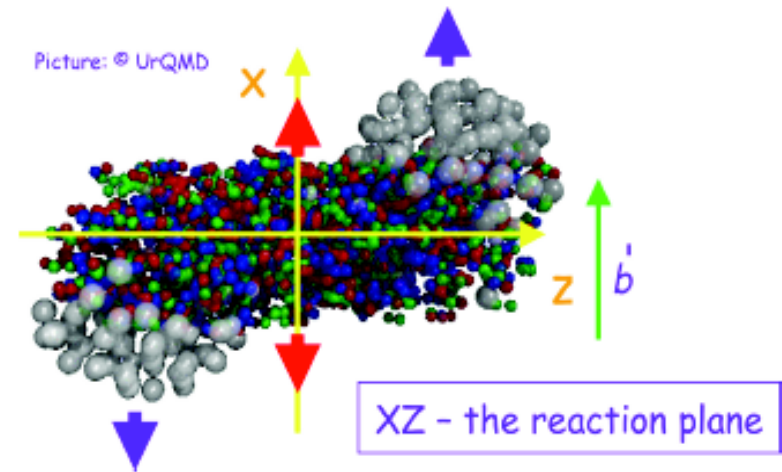
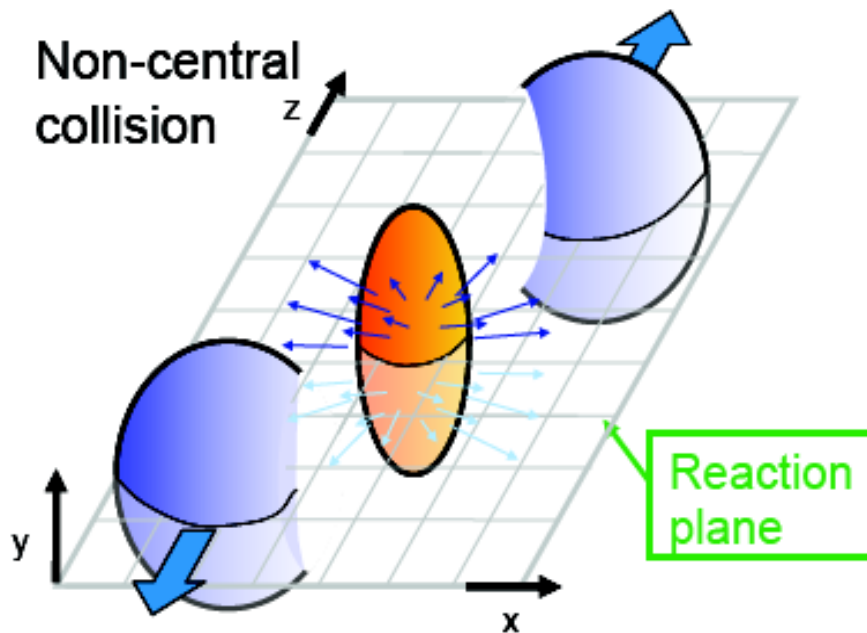
Resolve medium constituents (quarks and gluons)

Study spectra (e.g. transport coefficients, mean free path) quantities

The Experiments

- ALICE
 - Experiment designed for Heavy Ion collision
 - only dedicated experiment at LHC, must be comprehensive and able to cover all relevant observables
 - **VERY robust tracking** for p_T from **0.1 GeV/c** to **100 GeV/c**
 - high-granularity 3D detectors with many space points per track (**560 million** pixels in the TPC alone, giving 180 space points/track)
 - **very low material budget** (**< 10% X_0** in $r < 2.5$ m)
 - **PID** over a very large p_T range
 - use of essentially all known technologies: TOF, dE/dx, RICH, TRD, topology, EM calor.
 - Hadrons, leptons and photons + Excellent vertexing
- ATLAS and CMS
 - General-purpose detectors, optimized for hard processes
 - Excellent Calorimetry => Jets
 - Excellent dilepton measurements, especially at high p_T
 - Very large acceptance tracking

The geometry of a Heavy Ion Collision



“peripheral” collision ($b \sim b_{\max}$)
“central” collision ($b \sim 0$)

Number of participants (N_{part}):

number of incoming nucleons (participants) in the overlap region

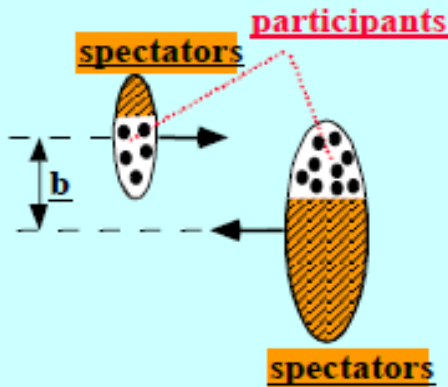
Number of binary collisions (N_{bin}):

number of equivalent inelastic nucleon-nucleon collisions

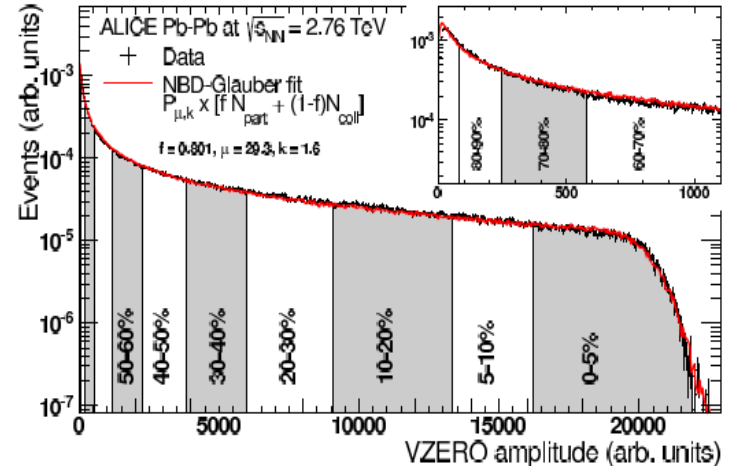
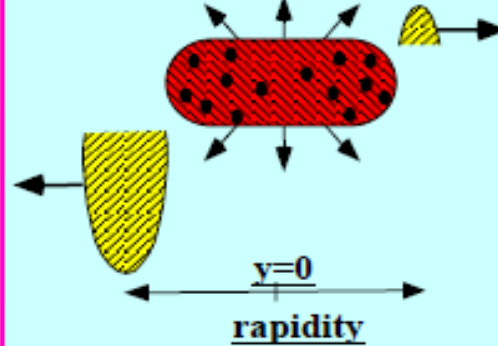
$$N_{\text{bin}} \approx N_{\text{part}}$$

More central collisions produce more particles

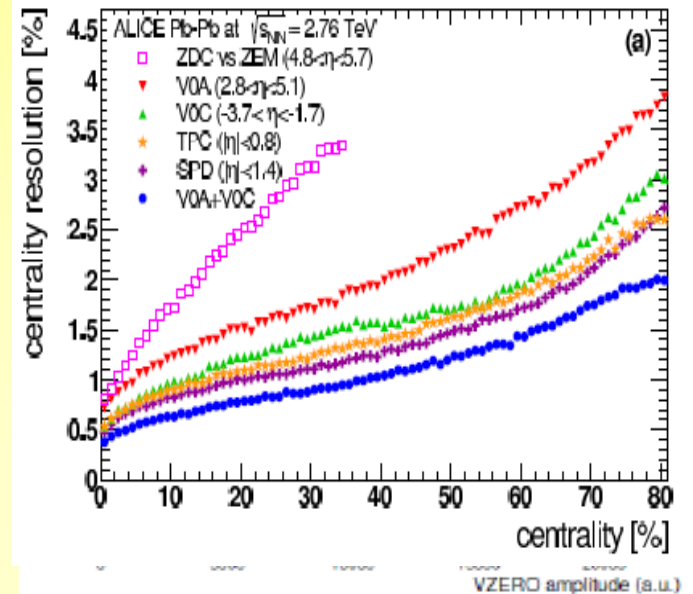
The geometry of a Heavy Ion Collision



$$y = \frac{1}{2} \ln \left(\frac{E + P_z}{E - P_z} \right)$$



arXiv:1301.4361



Centrality Determination

– Essential in all HI analysis, in ALICE based on correlation between:

- clusters measured in central rapidity region
- amplitudes of the signals in the forward region detectors:
 - VZERO scintillators $2.8 < \eta < 5.1$
 - $-3.7 < \eta < -1.7$

ZERO Degree Calorimeters

– With the full VZERO detector the resolution ranges from 0.5% in central collisions to 2% for peripheral

Kinematic Variables

Rapidity:
$$y = \frac{1}{2} \ln\left(\frac{E + P_Z}{E - P_Z}\right)$$

Pseudo-rapidity:
$$\eta = \frac{1}{2} \ln\left(\frac{P + P_Z}{P - P_Z}\right) = -\ln\left(\tan \frac{\theta}{2}\right)$$

Transverse Momentum:
$$p_T = \sqrt{p_X^2 + p_Y^2}$$

Transverse Mass:
$$m_T = \sqrt{p_T^2 + m_0^2}$$

Heavy Ions at the LHC

- Run1:

year	system	energy $\sqrt{s_{NN}}$ TeV	integrated luminosity
2010	Pb – Pb	2.76	$\sim 0.01 \text{ nb}^{-1}$
2011	Pb – Pb	2.76	$\sim 0.1 \text{ nb}^{-1}$
2013	p – Pb	5.02	$\sim 30 \text{ nb}^{-1}$

- Run2: (2015, 2016, 2017)
Pb-Pb 1 nb^{-1} at $\sqrt{s_{NN}}$ 5.1 TeV
p-Pb at $\sqrt{s_{NN}}$ 8.2 TeV

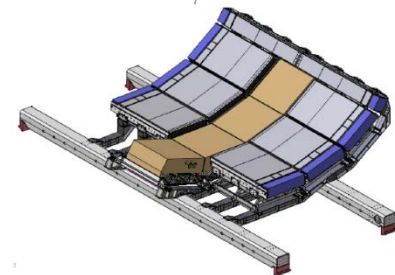
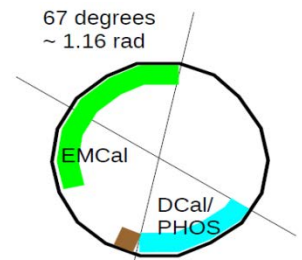
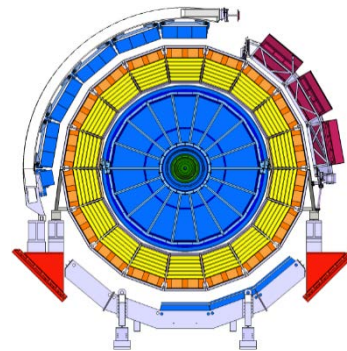
+ pp “reference” runs in 2010 and 2013 (2.76 TeV),
2015 (5.02 TeV).

LS2: Experiments and LHC upgrades

- Run3 + Run4 (2020, 21, 22): Pb-Pb 10 nb^{-1} at $\sqrt{s_{NN}}$ 5.5 TeV
with major detectors improvements
plus pPb.

LS1 New installations:

- 5 TRD modules
 - 8 Dcal modules
 - Add 1 PHOS module
 - Replacement of the whole DAQ/HLT,
 - New readout for the TPC
- And a major of consolidation effort all over

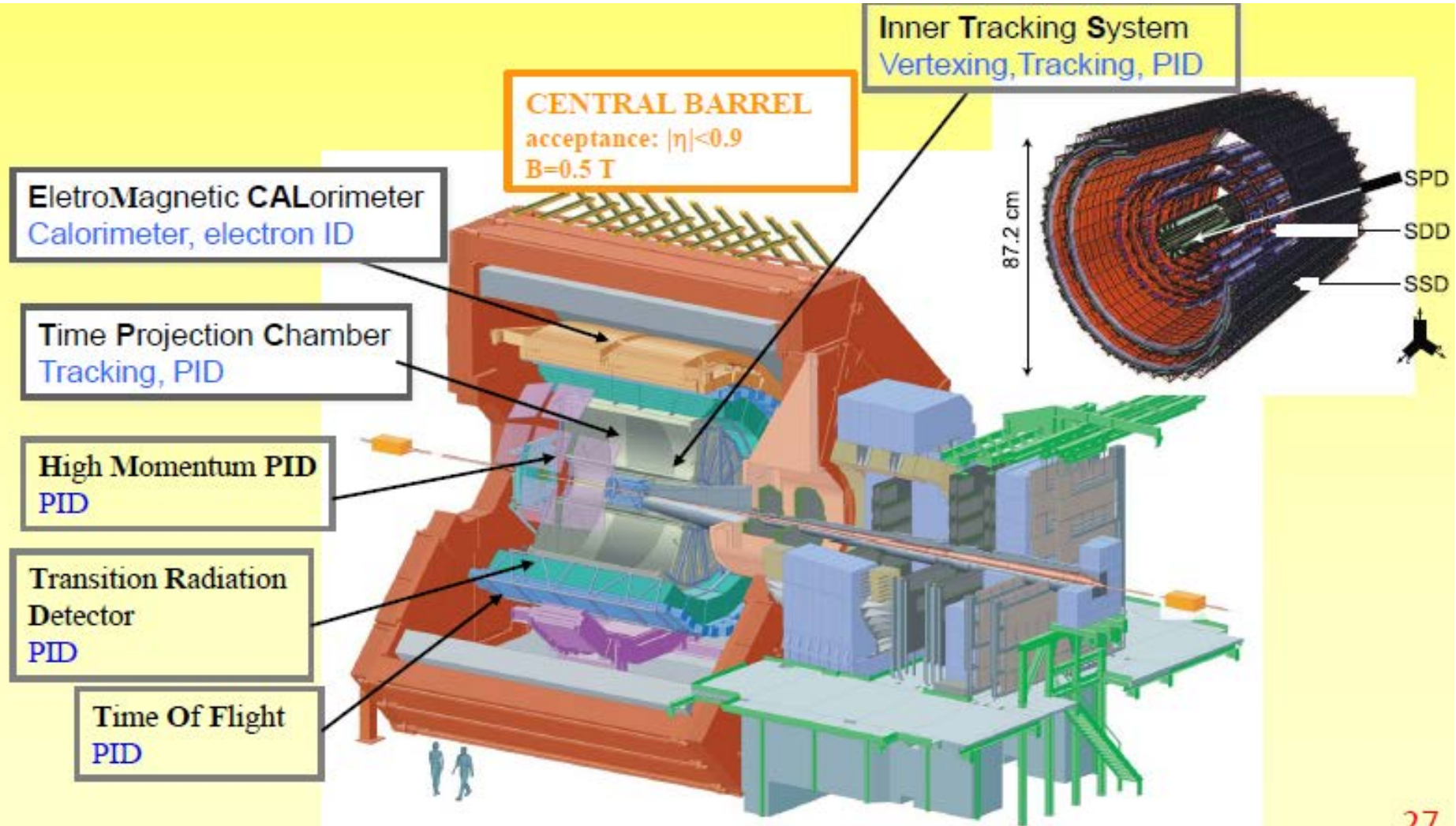


**Three phases, each jumping one order of magnitude in statistics
and progressively improving detectors**

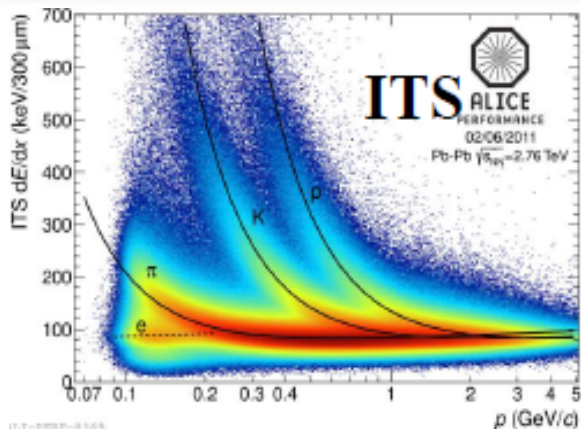
Alice detector

$$dN_{ch}/d\eta = 4000$$

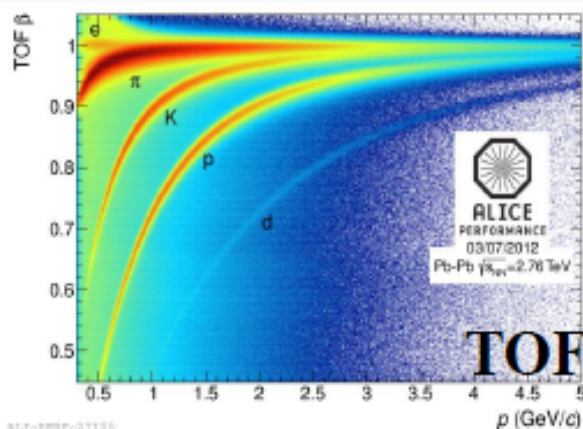
Excellent track and vertex reconstruction capabilities (TPC, ITS)
Particle identification over a wide momentum range



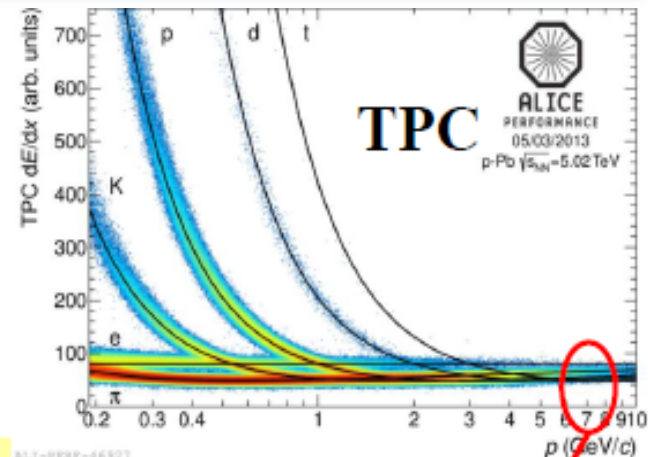
ALICE performance: PID



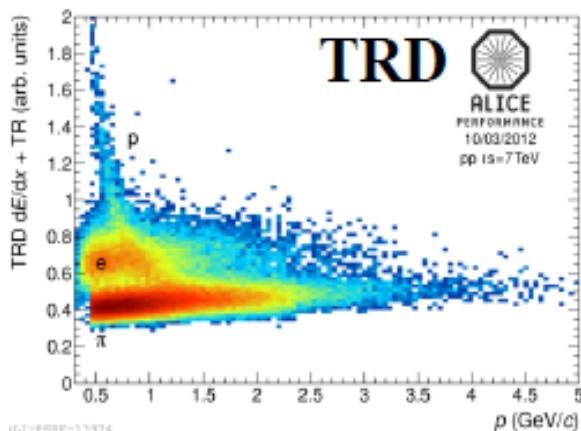
ALICE-PHOS-0369



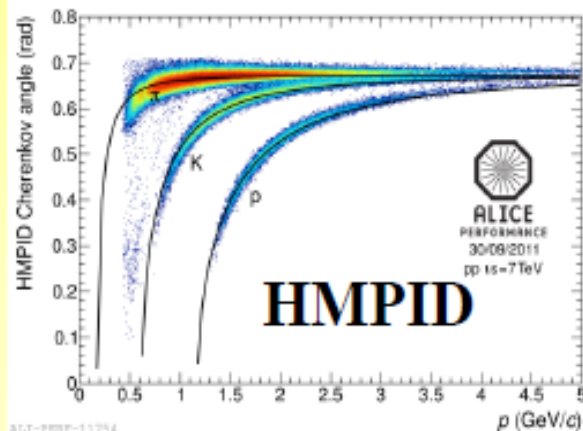
ALICE-PHOS-01125



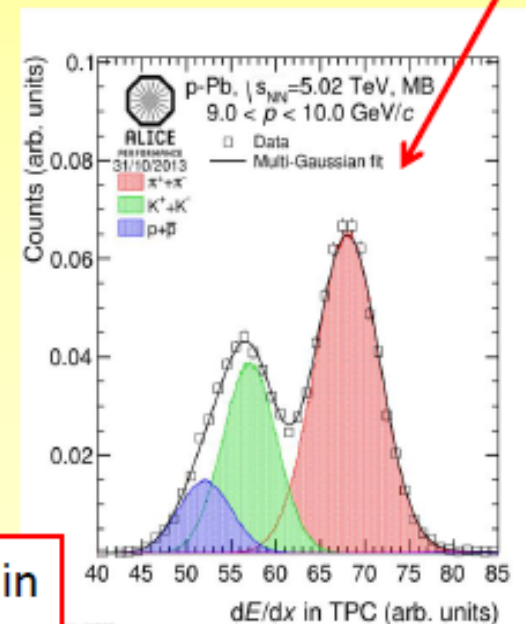
ALICE-PHOS-46927



ALICE-PHOS-13974



ALICE-PHOS-11754

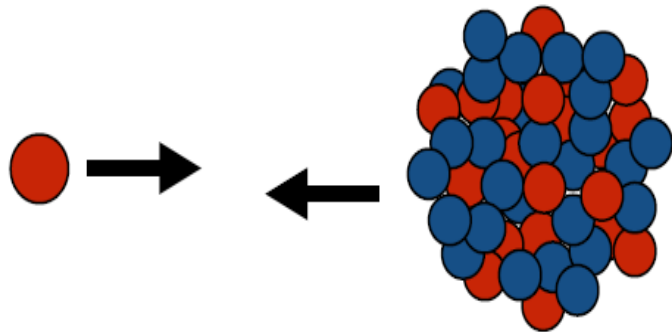


ALICE-PHOS-46927

- ALICE uses practically all known techniques

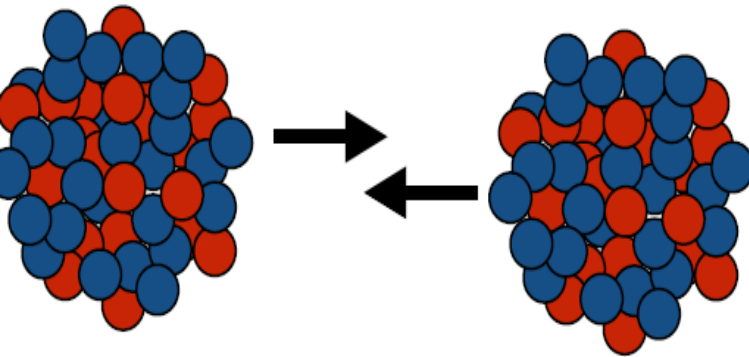
Statistical separation in relativistic rise region

p-A and AA collisions



Effects not due to QGP formation can modify the yield of hard probes in nuclear collisions (cold nuclear matter CNM):

- nuclear modification of the PDFs (shadowing at low Bjorken- x is the dominant effect at LHC energies)
- k_t broadening (due to multiple elastic collisions of the parton before the hard scattering)
- energy loss in CNM
- other FS effects?

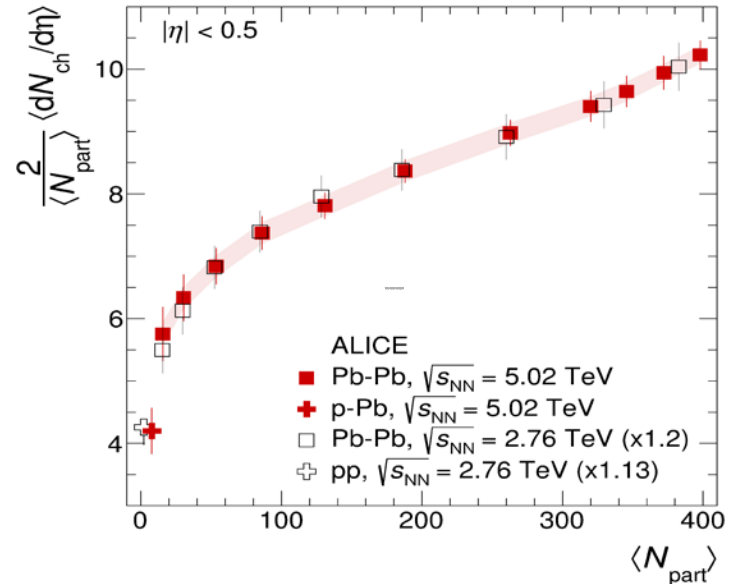
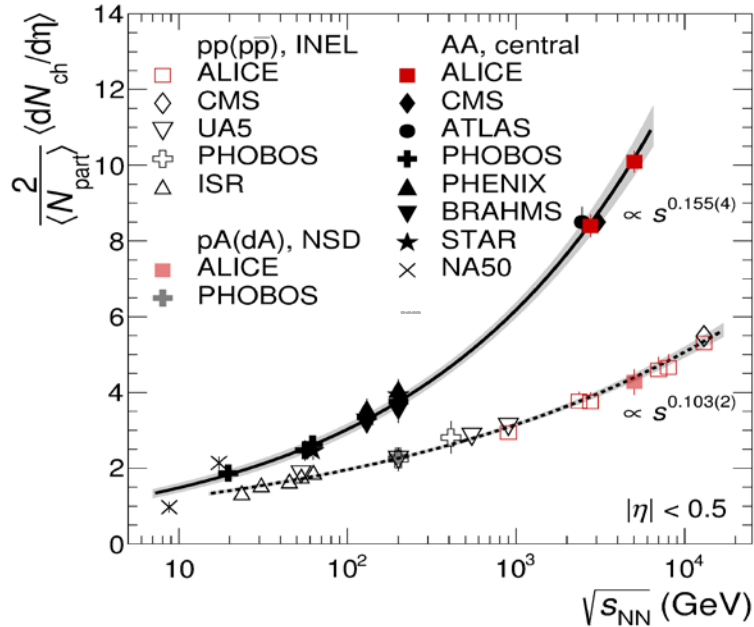


Hot nuclear matter: can be studied by

- Global observables and collective behaviour
 - *charged particle multiplicity*
 - *Flow*
- High p_T
 - *Charged particles*
 - *Jets*
- Open heavy flavors
- Quarkonia
 - *Charmonia*
 - *Bottomonia*

Charged particle multiplicity at midrapidity

ALICE Phys. Rev. Lett. 116 (2016) 222302



$\langle dN_{ch}/d\eta \rangle$ vs $\sqrt{s_{NN}}$ (0-5% most central collisions)

- Behaviour observed at lower energies confirmed
- Pb-Pb different from pp and pA
- 20% increase for Pb-Pb from 2.76 to 5.02 TeV

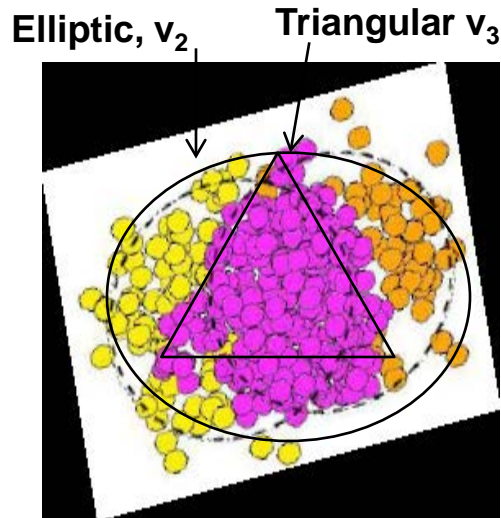
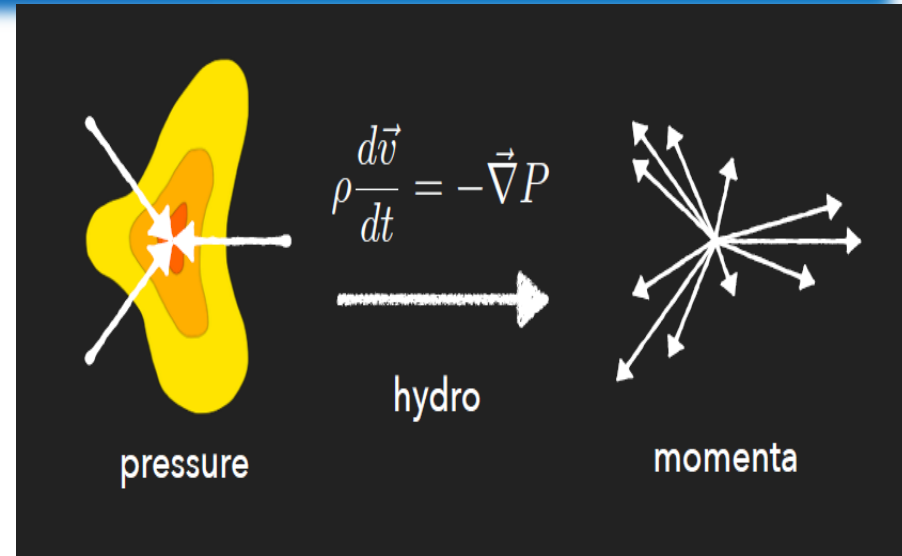
$\langle dN_{ch}/N_{part} \rangle$ vs N_{part}

- Shape very similar to the one observed at lower energy AA collisions.
- Increase with a factor 1.8 from peripheral to central AA collisions.

Anisotropic Flow

- **Azimuthal anisotropy** of emitted particles
 ← pressure gradient ← initial space anisotropy of the overlap region
- **Quantified by** Fourier decomposition of particle azimuthal distribution relative to the reaction plane
- **Sensitive to** hydrodynamic properties of the expanding medium

$$E \frac{d^3 N}{d^3 p} = \frac{1}{2\pi} \frac{d^2 N}{p_t dp_t dy} \left[1 + \sum_{n=1}^{\infty} 2v_n \cos(n\phi) \right]$$



Main message from lower energies studies (RHIC, LHC RUN1)

- ✓ Values of flow coefficients are large
- ✓ In the transition from RHIC to LHC energies elliptic flow v_2 increases by 30% as predicted by hydrodynamic model that include viscous corrections.

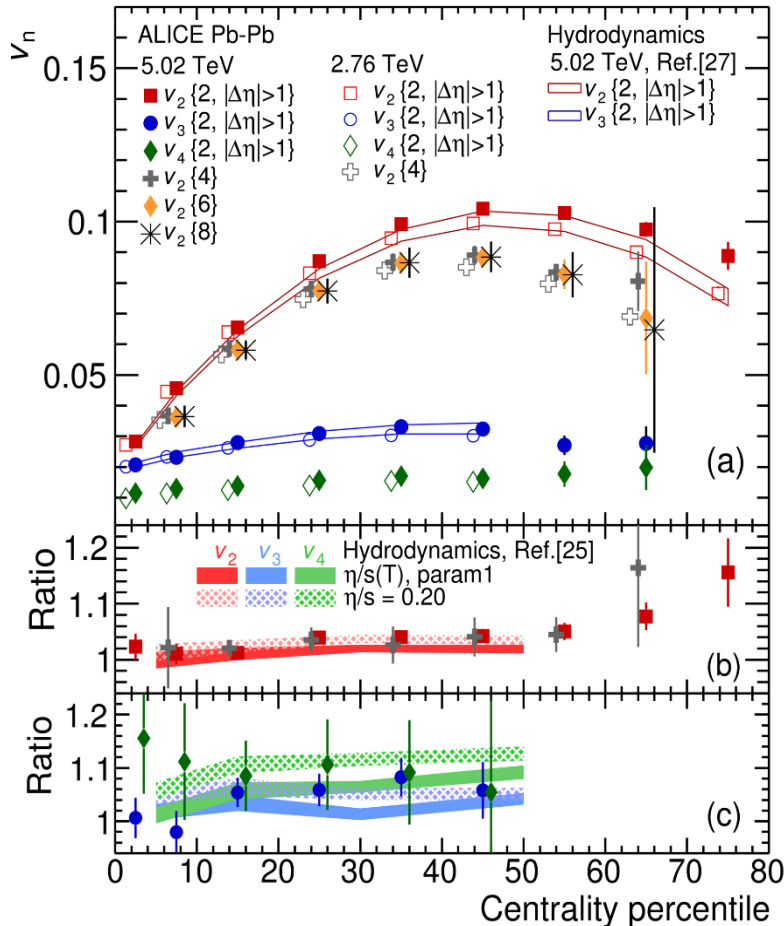
Indication for a strongly interacting, low viscosity «perfect» fluid.

Anisotropic Flow

Results at 5.02 TeV: centrality and energy dependence of flow coefficients

Phys. Rev. Lett. 116, 132302 (2016)

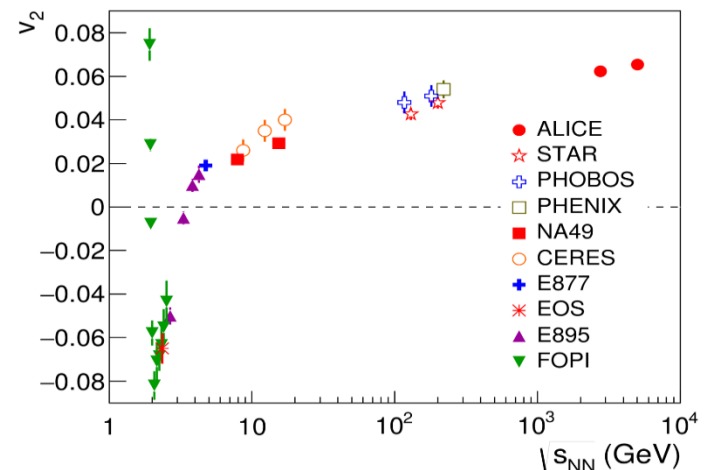
Centrality dependence: results at 5.02 TeV and 2.76 TeV



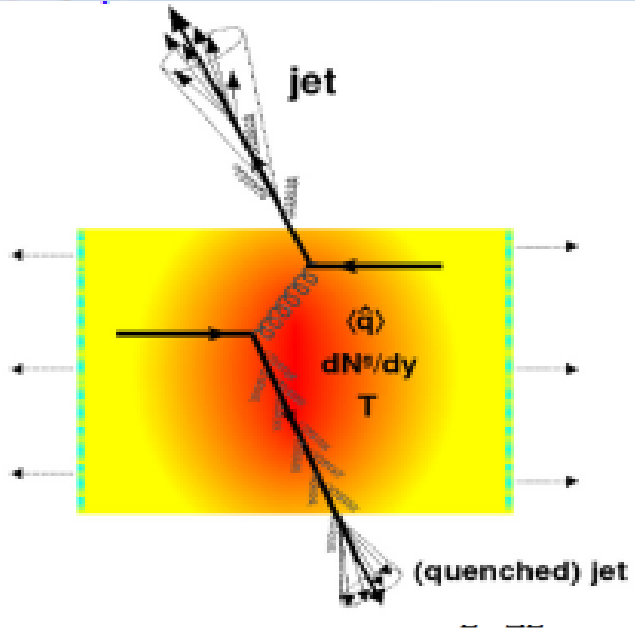
- ✓ Increase (by 3%, 4.3%, 10.2%) for v_2 , v_3 , v_4 in 0-50% centrality from 2.76 to 5.02 TeV.
- ✓ Ratio (5.02 and 2.76 TeV) sensitive to shear viscosity-to-entropy ratio (η/S), (constraint to theoretical calculations) \rightarrow data indicate no or small changes in η/S with energy.

Energy dependence of v_2 (20%-30% centrality)

- ✓ Increase predicted by hydrodynamic models



High- p_T hadrons and Jets



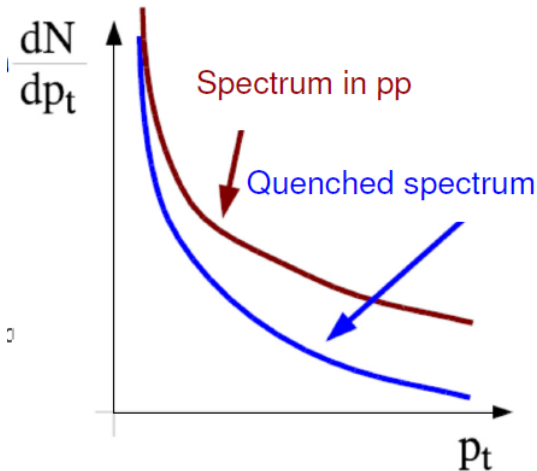
Parton energy loss:

a parton passing through the QCD medium undergoes energy loss which results in the suppression of high- p_T hadron yields, via

- Collisional energy loss with partons in the medium
- Radiation of gluons (gluonstrahlung)

Experimental observable:

Nuclear Modification Factor R_{AA}



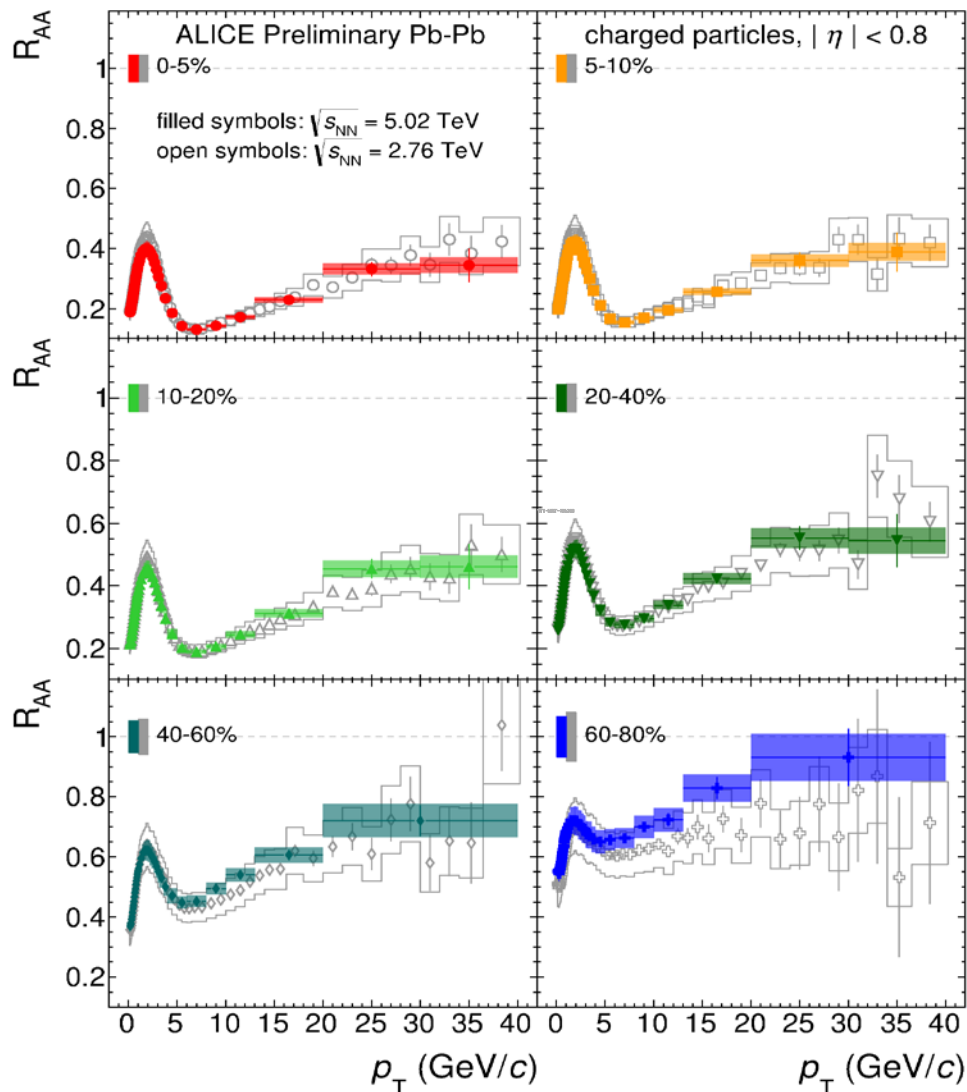
$$R_{AA}(p_T) = \frac{1}{\langle N_{coll} \rangle} \frac{dN_{AA} / dp_T}{dN_{pp} / dp_T}$$

QCD medium

QCD vacuum

Binary nucleon-nucleon collisions

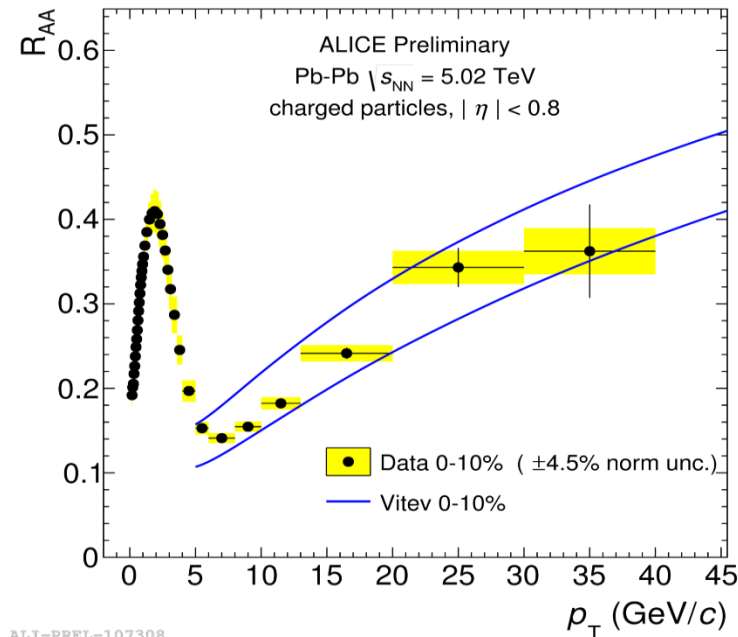
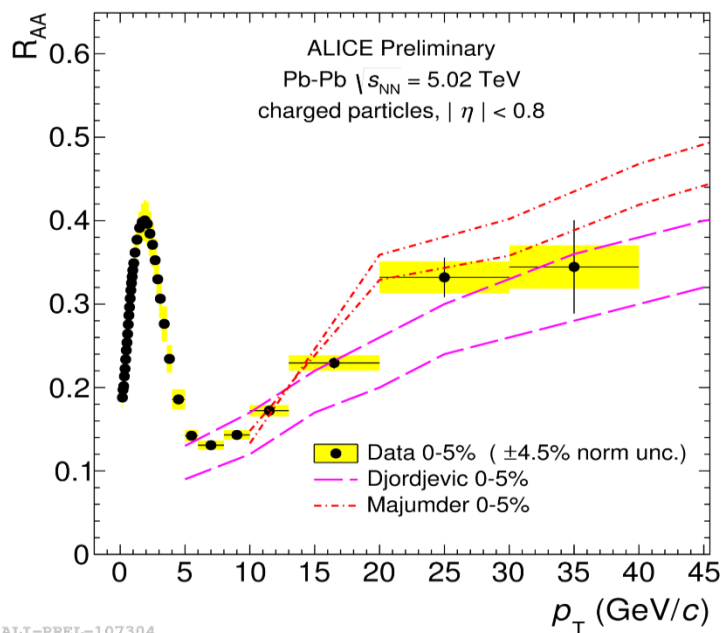
R_{AA} of high p_T charged particles



- Nuclear modification factor R_{AA} for non-identified charged particles measured at mid rapidity in different centrality bins
 - Strong suppression of charged particle production confirmed
 - R_{AA} at 5.02 TeV similar to 2.76 TeV
 - Minimum at $p_T \approx 6-7$ GeV/c
 - Rise in the p_T region between 6 and 50 GeV/c
 - Clear evolution with centrality
- More central collisions: longer path length, denser medium lead to more suppression**

R_{AA} of high p_T charged particles

R_{AA} : comparison to models



Data reproduced by models including:

Radiative energy loss

Vitev et al., Phys. Rev. D 93 074030 (2016)

Majumder et al., Phys. Rev. Lett. 109 202301 (2016)

Radiative and collisional energy loss

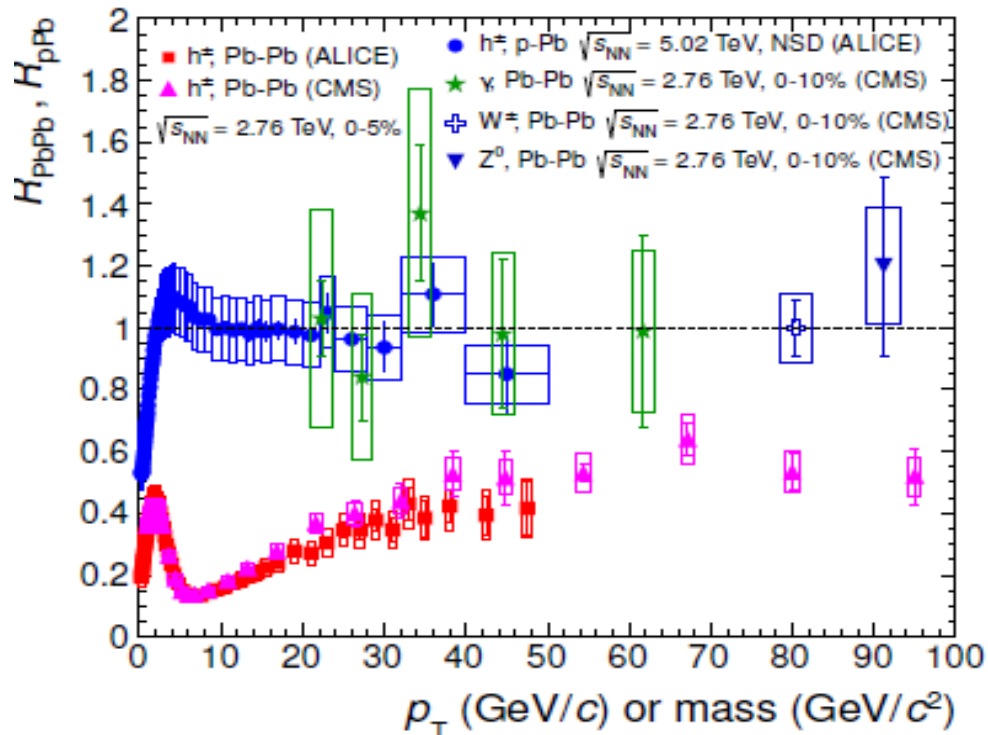
Djordjevich et al., arXiv:1601.07852

Rise of R_{AA} constrains energy loss mechanism (relative loss decreases with p_T)

R_{AA} in p Pb for charged hadrons

- R_{pA} expected to be sensitive to **initial** state, but not to **final** state effects.

ALICE PRL 110(2013) 082302



$$R_{pA} = \frac{dN_{pA} / dp_T}{\langle N_{coll} \rangle dN_{pp} / dp_T}$$

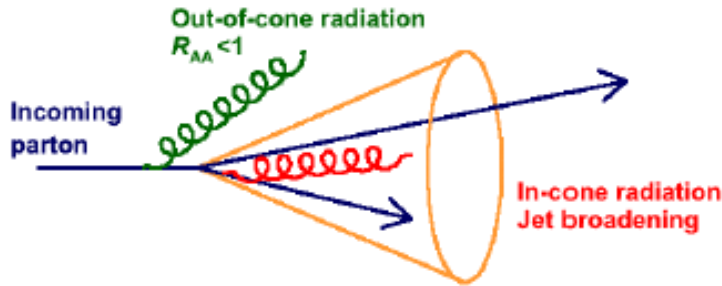
R_{pPb} consistent with unity for $p_T > 2 \text{ GeV}/c$.

- Small Cronin-like enhancement visible at low p_T .
- Consistent with R_{AA} of particles which are not sensitive to QGP dynamics (γ , W^\pm , Z^0).

The strong suppression of hadron production at high p_T in nucleus-nucleus collisions is not due to an initial-state effects.

-Evidence of parton energy loss

Jets



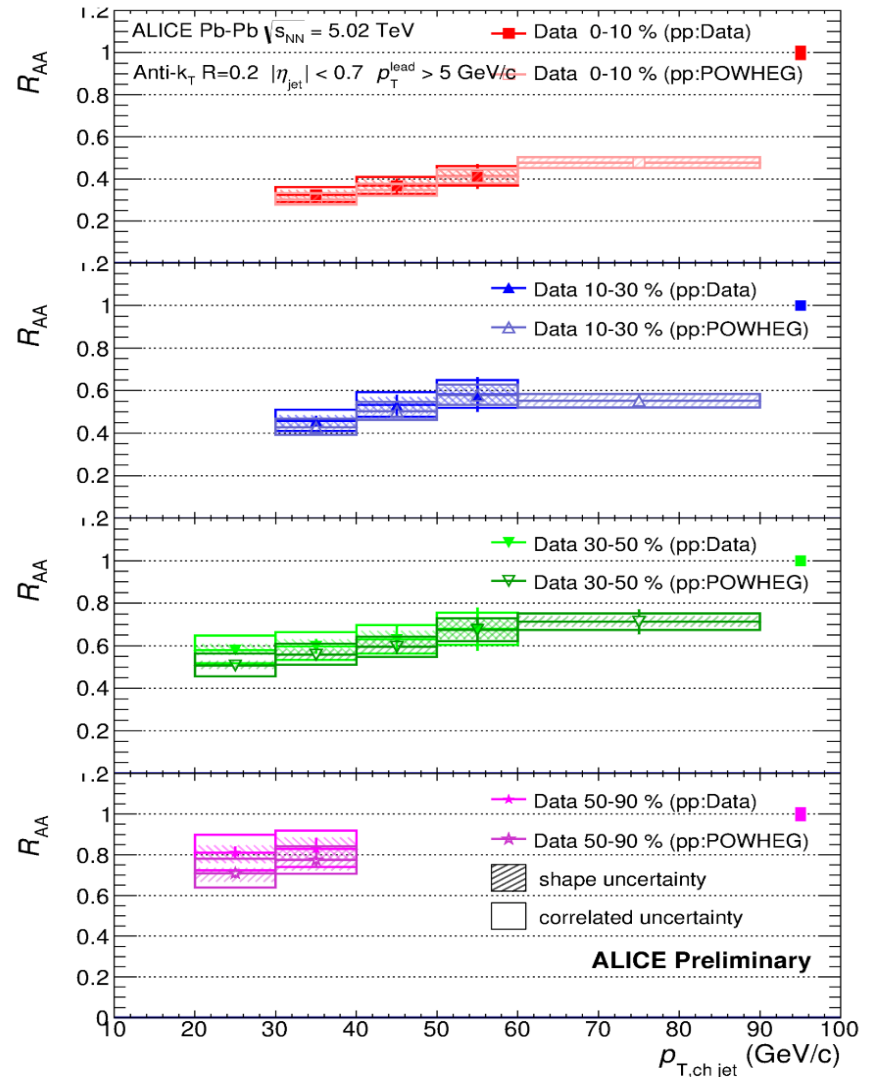
Jets: spray of particles from hard parton fragmentation \rightarrow closer access to parton energy

Out of cone radiation \rightarrow influence on Jet R_A

In-cone radiation \rightarrow may lead to Jet shape modifications, «jet broadening»

Charged-particle jet R_{AA} :
Strong suppression observed at **5.02 TeV**

- Clear evolution with centrality



ALI-PREL-113513

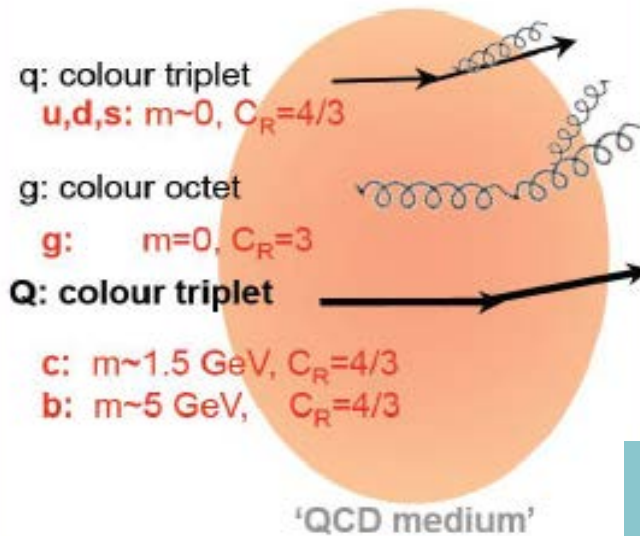
Open heavy flavors

- Large mass ($m_c \approx 1.5$ GeV, $m_b \approx 5$ GeV) \rightarrow produced in hard processes at the initial stage of the collision with short formation time, much smaller than QGP lifetime
- Flavor conserved by strong interaction + production of HF in QGP is subdominant \rightarrow interaction with QGP do not change flavor identity



HF are hardly destroyed/created by the medium and are transported through the full system evolution

Tool for understanding the general properties of parton energy loss in a deconfined medium since this is expected to depend (also) on the Casimir factor C_R and on the quark mass (dead cone effect)



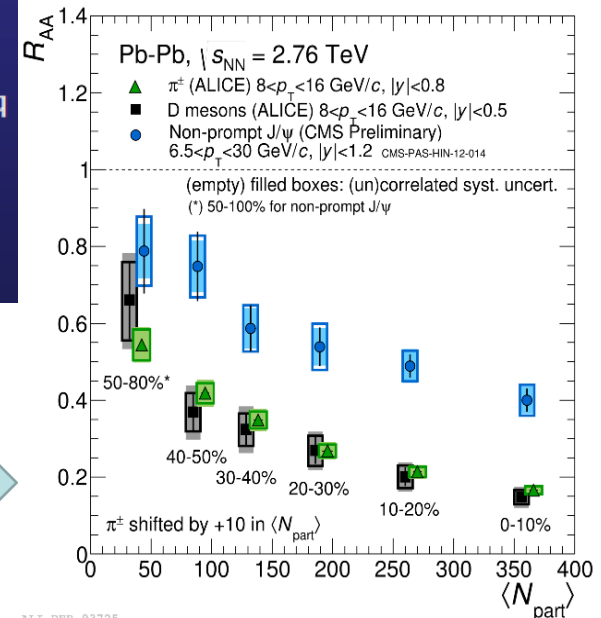
$$\Delta E_{\text{quark}} < \Delta E_{\text{gluon}}$$

$$\Delta E_b < \Delta E_c < \Delta E_{\text{light } q}$$

which should imply

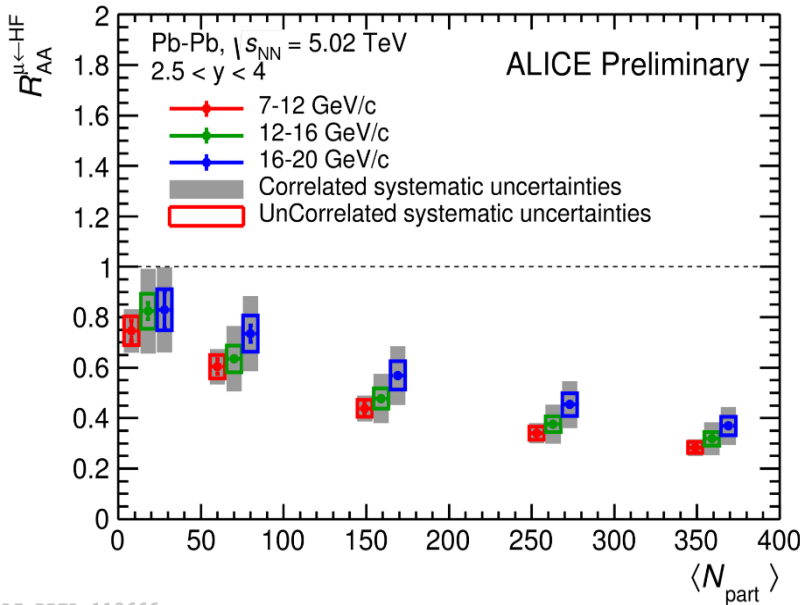
$$R_{AA}^B > R_{AA}^D > R_{AA}^\pi$$

RUN-I: first indication of mass dependence of energy loss



Open heavy flavors

First R_{AA} results at 5.02 TeV: muons from HF decays at forward rapidity

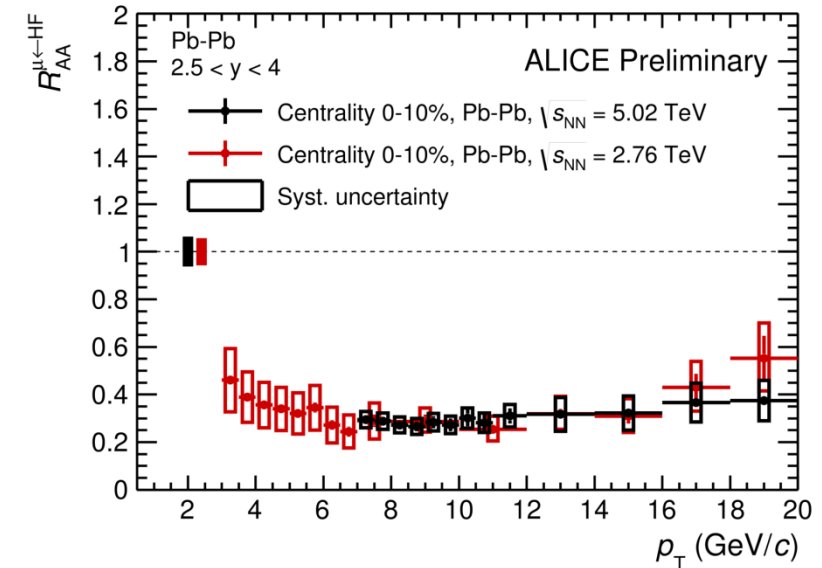


ALI-PREL-113666



Strong suppression of muons from HF decay:

- increasing with centrality
- (slightly) decreasing with p_T for p_T above 7 GeV/c



ALI-PREL-113642

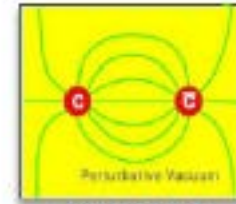


R_{AA} at 5.02 TeV is compatible with the one at 2.76 TeV
 (note: denser medium but flatter p_T spectrum)

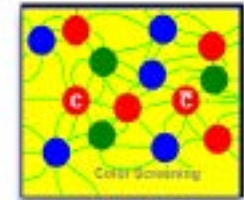
Quarkonia suppression and re-generation

- Matsui & Satz: charmonia are dissociated in QGP because of color screening $\rightarrow J/\psi$ suppression
- The **screening radius** $\lambda_D(T)$ (i.e. the maximum distance which allows the formation of a bound QQ pair) decreases with the temperature $T \rightarrow$ Difference between binding energies of quarkonia states

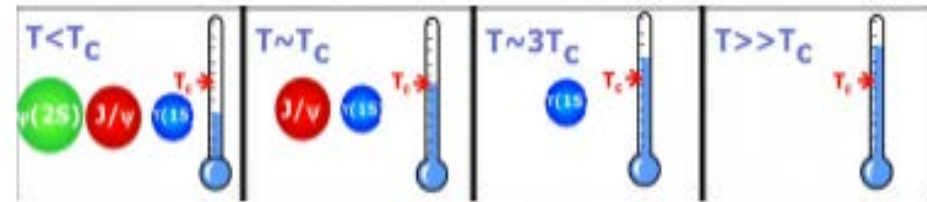
\rightarrow sequential melting, QGP Thermometer
(Digal, Petrecki, Satz PRD 64(2001) 0940150)



In vacuum



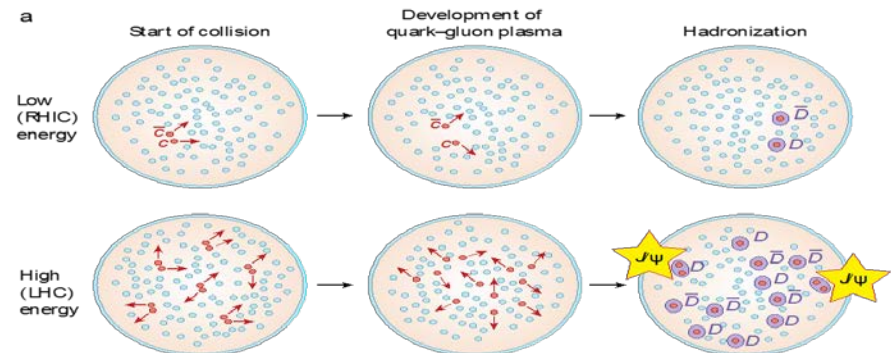
In QGP



Increasing the energy of the collision, the $c\bar{c}$ pair multiplicity increases and may lead to **charmonium production via recombination**

In most central A-A collisions	SPS 20 GeV	RHIC 200 GeV	LHC 2.76 TeV
$N_{c\bar{c}}/\text{event}$	~ 0.2	~ 10	~ 60

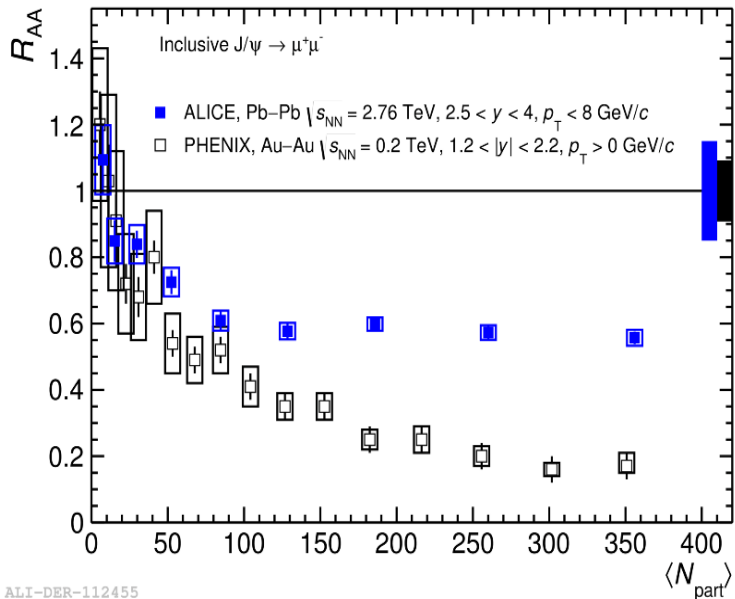
Charmonium production may be enhanced via (re)combination of cc pairs at hadronization (statistical approach) or during QGP stage (kinetic recombination approach)



J/ψ : R_{AA} vs centrality

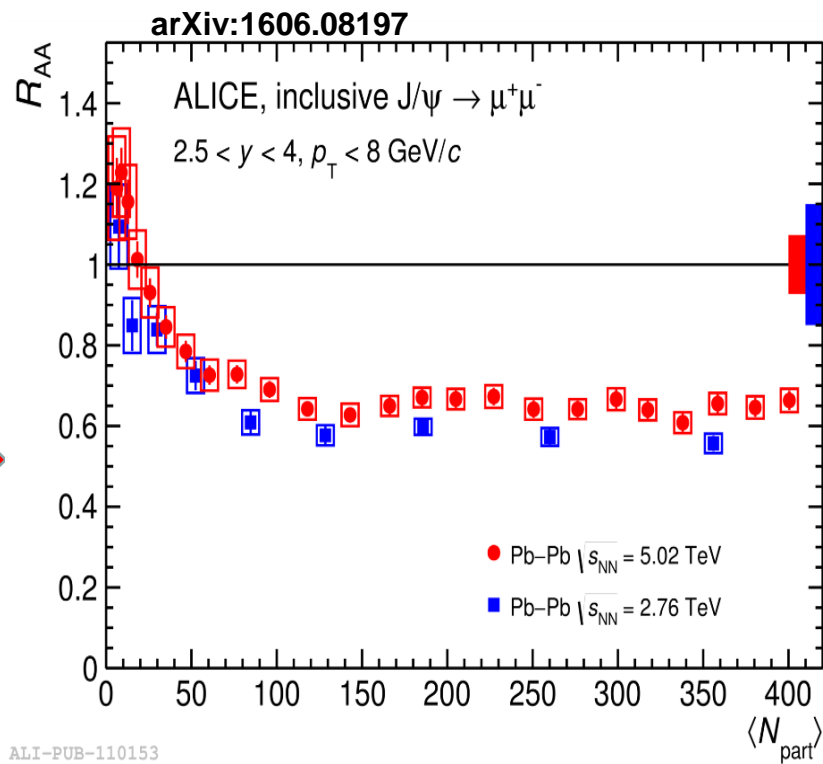
PLB 734 (2014) 314-327

Focus: inclusive J/ψ prod. at forward rapidity



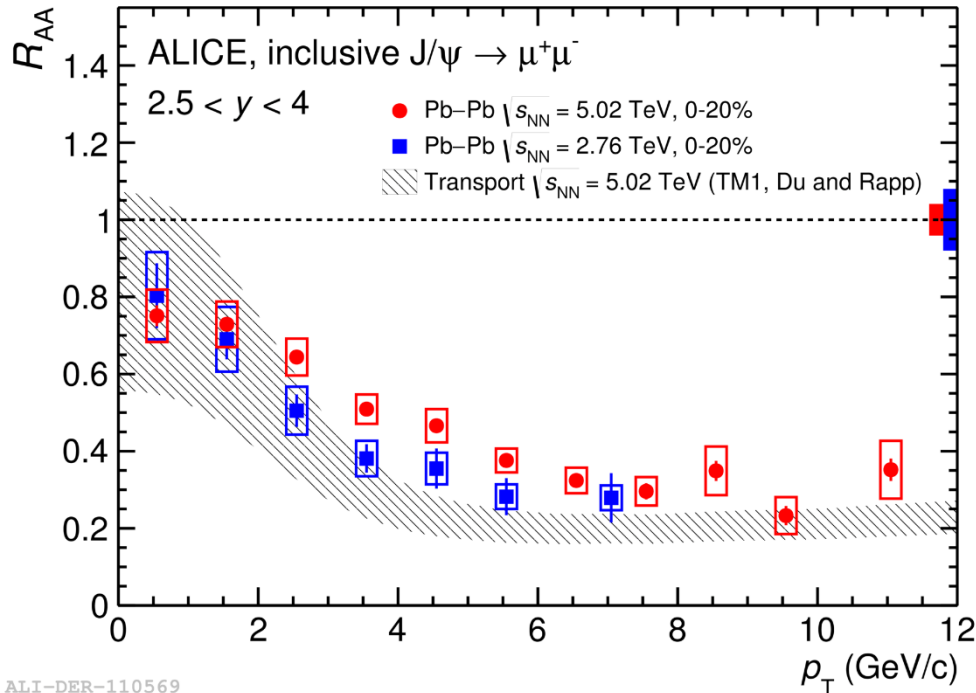
- **R_{AA} in Pb-Pb collisions at 2.76 TeV:**
 - ✓ Larger than Au-Au collisions at 200 GeV:
 - ✓ J/ψ less suppressed at LHC than at RHIC
 - ✓ Consistent with regeneration scenarii

- **R_{AA} in Pb-Pb collisions at 5.02 TeV:**
 - ✓ w.r.t. RUN I: better statistics and reduced systematics errors
 - ✓ Trend similar to the one at 2.76 TeV
 - ✓ Flat behaviour for N_{part} > 100
 - ✓ Hint for electromagnetic production in the most peripheral bins



J/ψ : R_{AA} vs p_T

Comparison to 2.76 TeV and to models



ALI-DER-110569

Extended p_T range at 5.02 TeV, up to 12 GeV/c

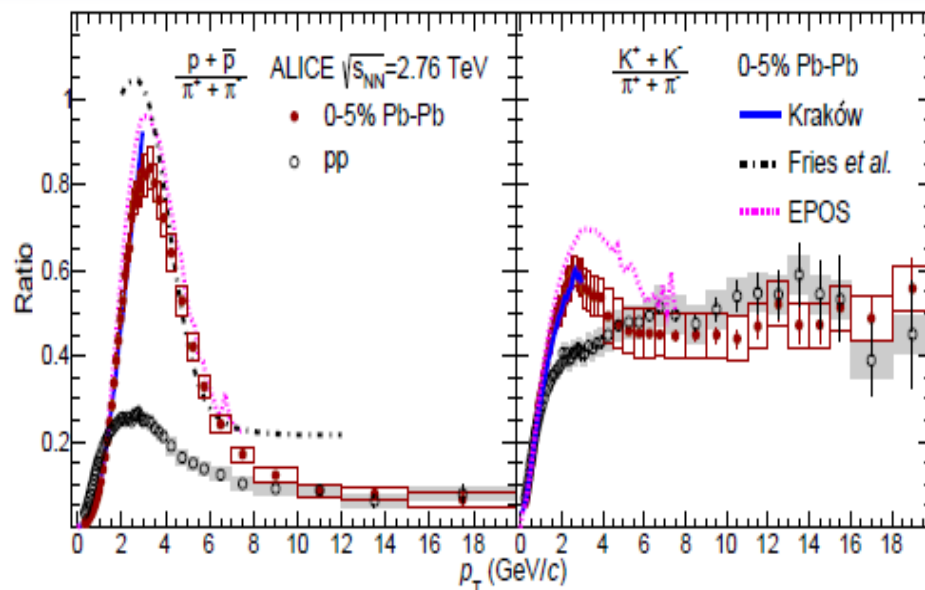
In the common p_T interval, similar behaviour for the two energies.

We observe less suppression at low p_T , as expected in case of a strong regeneration component

The observed behavior is reasonably well reproduced by transport models (Du and Rapp)

Particle ratio and $R_{p_bP_b}$ for identified light flavor hadron

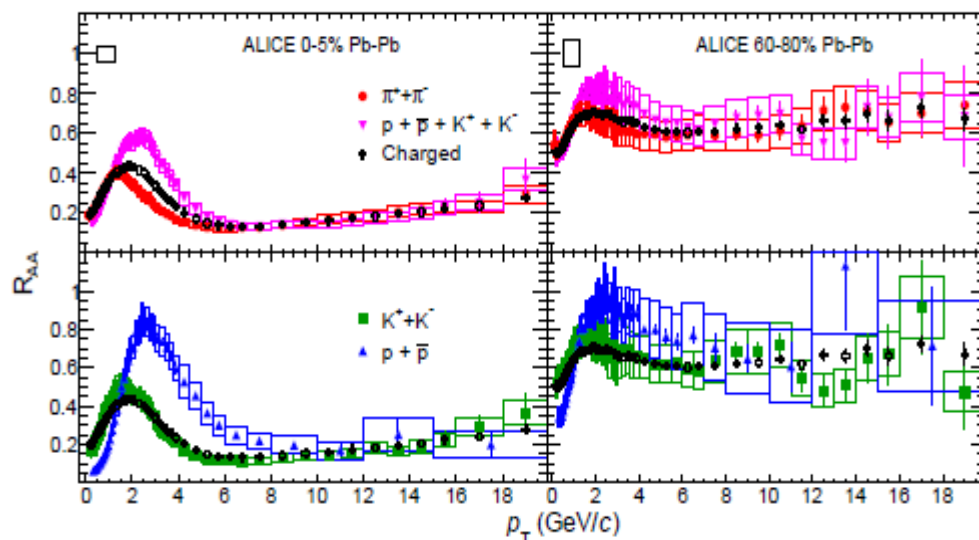
PLB 736 (2014) 196



At intermediate p_T Cronin region:
Indication of mass ordering

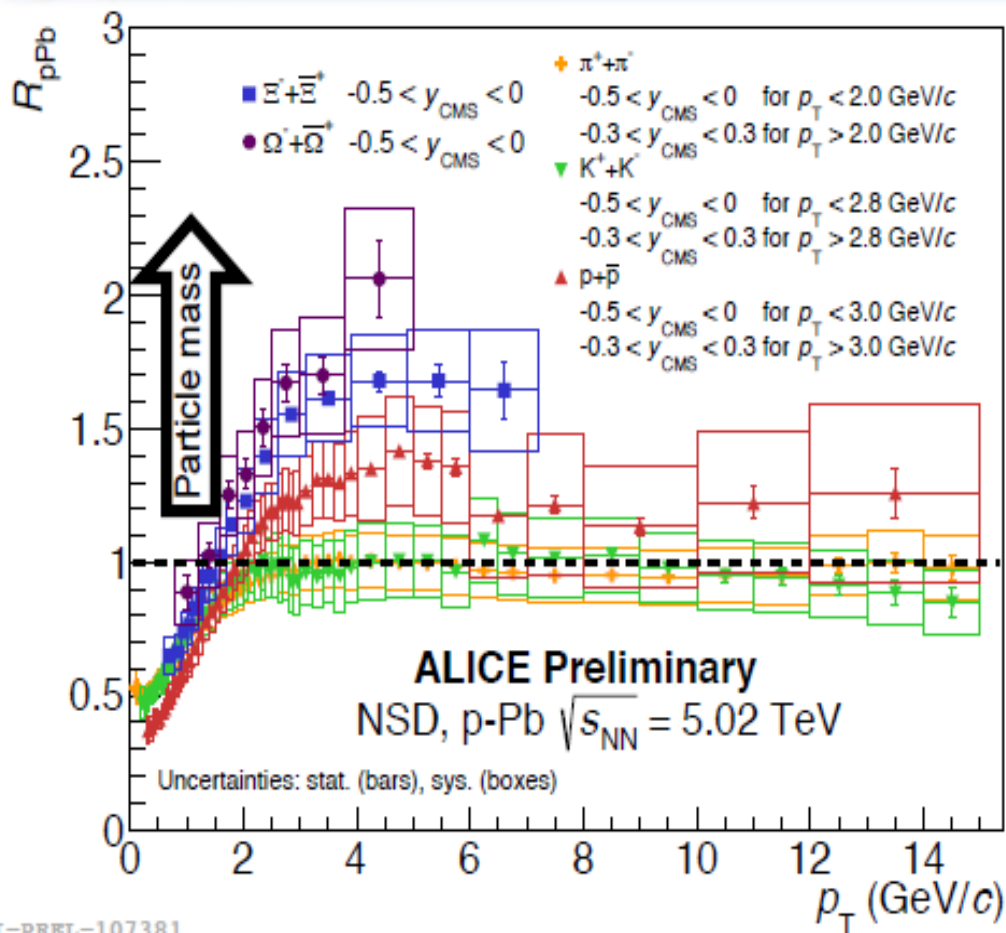
- Pronounced peak for **protons**
- **Clear peak for Kaons**
- The Krakow hydrodynamical model well describe the rise of the peak
- EPOS generator hydro+hadronization tends to overestimate the peak

At $p_T > 10$ GeV/c ratios like those in pp



- For $p_T < 10$ GeV/c protons less suppressed than kaons and pions.
- For $p_T > 10$ GeV/c all particle species are equally suppressed \rightarrow the particle composition and ratios at high p_T are similar to those in vacuum.

R_{pPb} for identified light flavor hadrons



At intermediate p_T Cronin region:
Hint of mass ordering

- No enhancement for **pions and kaons**
- Pronounced peak for **protons**
- Even stronger for **heavier mass**.

Mass ordering can be connected to collective behaviour (flow-like effects) in p-Pb collisions?

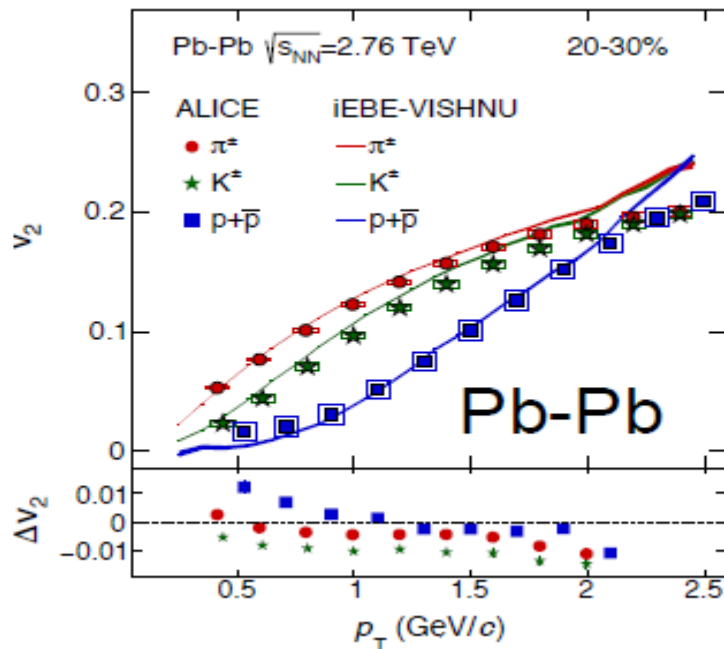


Particles specie dependences point to relevance of final-state effects

Long-range angular correlation of π , K and p and v_2 for identified hadrons in p-Pb

Correlation between trigger h and identified hadron.

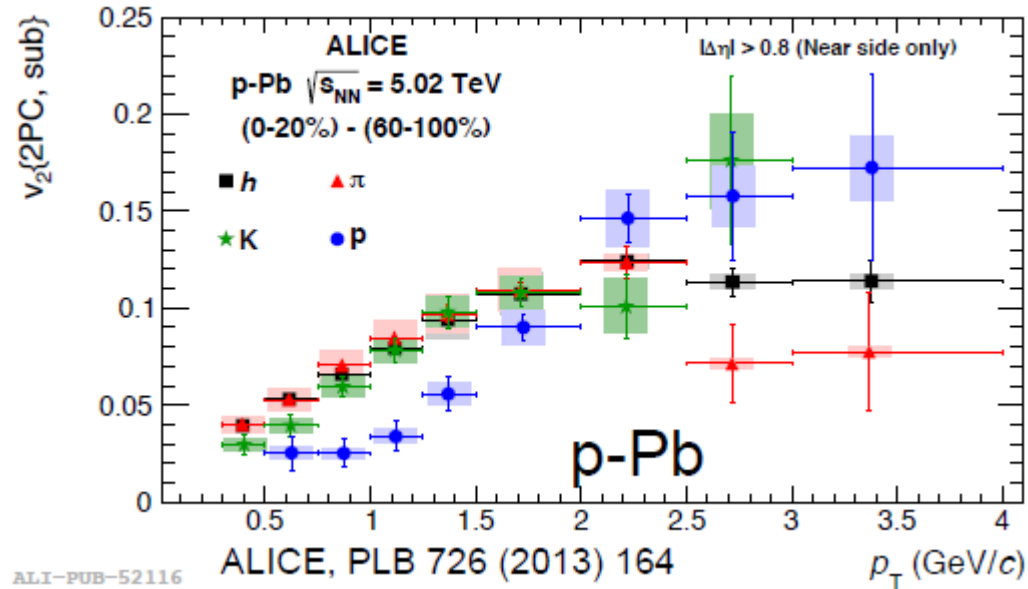
Jet correlation subtracted.



ALI-PUB-109488

Double-ridge structure with a near side ridge at $\Delta\phi=0$ and away-side at $\Delta\phi=\pi$ observed for h, π , k and p
Resembling what seen in Pb-Pb

Fourier decomposition: v_2 vs p_T



$$V_2^\pi \sim V_2^K$$

$$V_2^p < V_2^\pi \text{ at } p_T < 2 \text{ GeV}$$

$$V_2^p > V_2^\pi \text{ at } p_T > 2 \text{ GeV}$$

Large v_2 values!

Mass ordering similar to Pb-Pb, where data are reproduced by hydrodynamical models.

Summary

Hot QCD

- Strong **jet quenching** at high $p_T \rightarrow$ energy loss of partons in QGP: wealth of data from leading particles and reconstructed jet.
- **Recombination mechanism** at low p_T
- **v_2 mass ordering** for light and strange hadrons up to $p_T < 2.5$ GeV/c

Pb-Pb a very hot system pointing to a QGP strongly interacting liquid....

"Cold" QCD –

- **No indications of quenching** at high p_T (charged hadrons, jets, open charm, heavy flavor electrons and muons). ...
- **Pb-Pb-like features** at low p_T (baryon/meson enhancement, double ridge, v_2 , ...) several indications supporting final state effects

p-Pb seems hotter than we thought

Enhanced production of multi-strange hadrons in high-multiplicity proton-proton collisions

ALICE Collaboration¹

p-p $\sqrt{s_{NN}} = 7$ TeV
p-Pb $\sqrt{s_{NN}} = 5.02$ TeV
Pb-Pb $\sqrt{s_{NN}} = 2.76$ TeV

Ratio of the yields of strange and multistrange to the pion
 Compared to p-Pb and Pb-Pb results

Significant enhancement of strange to non-strange hadron production vs multiplicity in p-p.

The behaviour in pp resembles that of p-Pb

At high multiplicity the yield ratios reach values similar to the ones observed in Pb-Pb

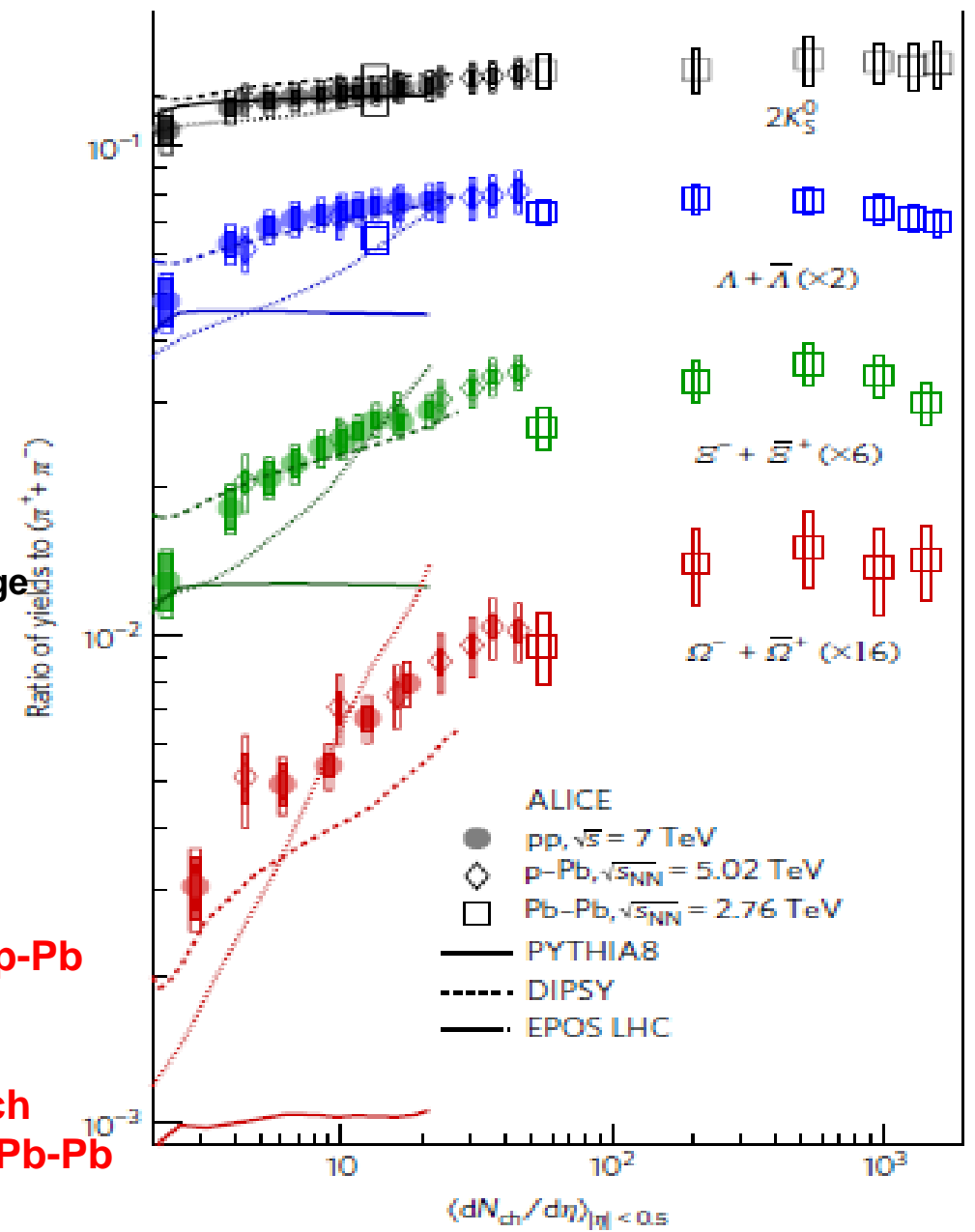


Figure 2 | p_T -integrated yield ratios to pions ($\pi^+ + \pi^-$) as a function of $\langle dN_{ch}/d\eta \rangle$ measured in $|y| < 0.5$. The error bars show the statistical

Enhanced production of multi-strange hadrons in high-multiplicity proton-proton collisions

ALICE Collaboration†

Particle yield ratios to pions normalized to the values measured in the inclusive INEL>0 pp sample: Show the evolution of the production of strange hadrons with multiplicity.

The observed multiplicity dependence enhancement follows a hierarchy determined by the hadrons strangeness rather than by mass or baryonic number of the hadron.

Such behaviour can not be reproduced by any of MC models.

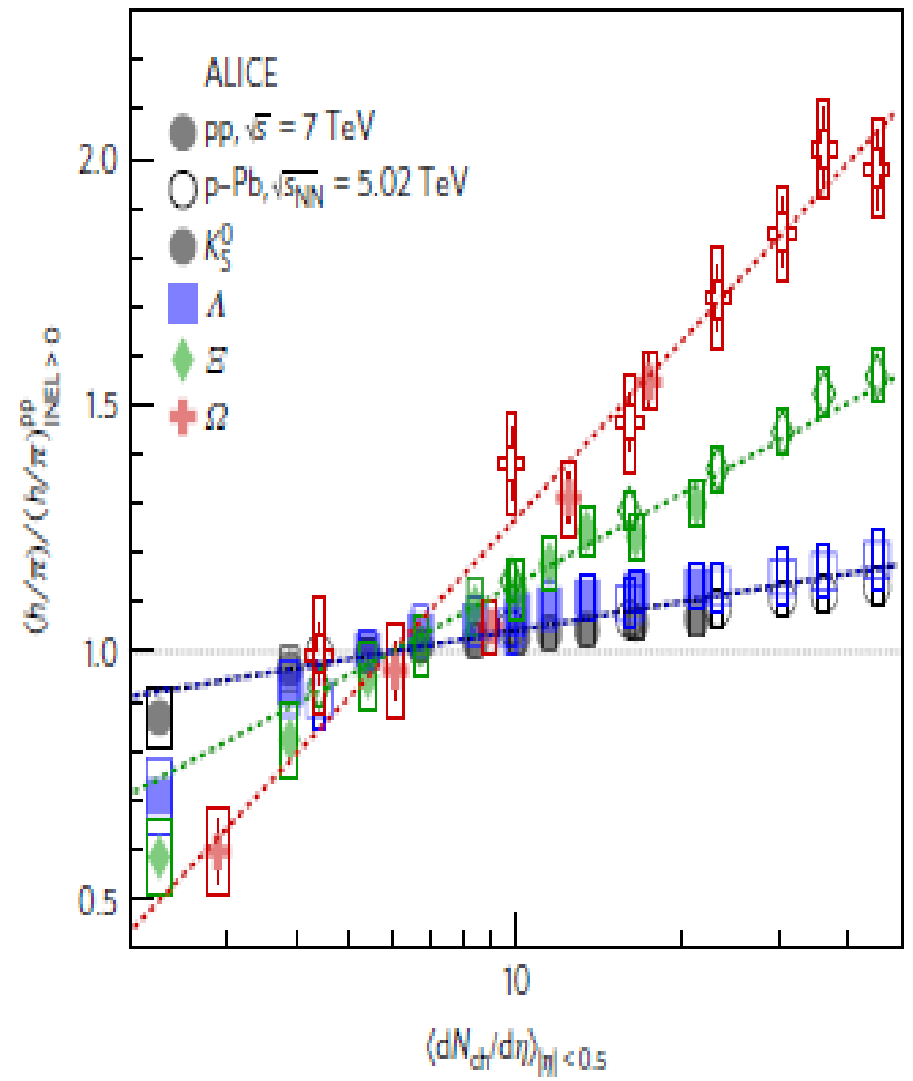


Figure 4 | Particle yield ratios to pions normalized to the values measured in the inclusive INEL > 0 pp sample. The results are shown for pp and

Run3: Detailed characterization of QGP

Progress on the characterization of QGP properties:

- precision measurements of **rare probes**
- over a large kinematic range: **from high to very low p_T**
- as function of multi-differential observables: **centrality, reaction plane,...**

Example: Precision measurements of spectra, correlations and flow of heavy flavors hadrons and quarkonia at low p_T .

Upgrade strategy focus on physics observables where ALICE detector unique features are essential:
PID, low material thickness, precise vertexing and tracking down to low p_T .

The LS2 ALICE Upgrades

New Inner Tracking System (ITS)

- improved pointing precision
- less material -> thinnest tracker at the LHC

Muon Forward Tracker (MFT)

- new Si tracker
- Improved MUON pointing precision

MUON ARM

- continuous readout electronics

Time Projection Chamber (TPC)

- new GEM technology for readout chambers
- continuous readout
- faster readout electronics

New Central Trigger Processor

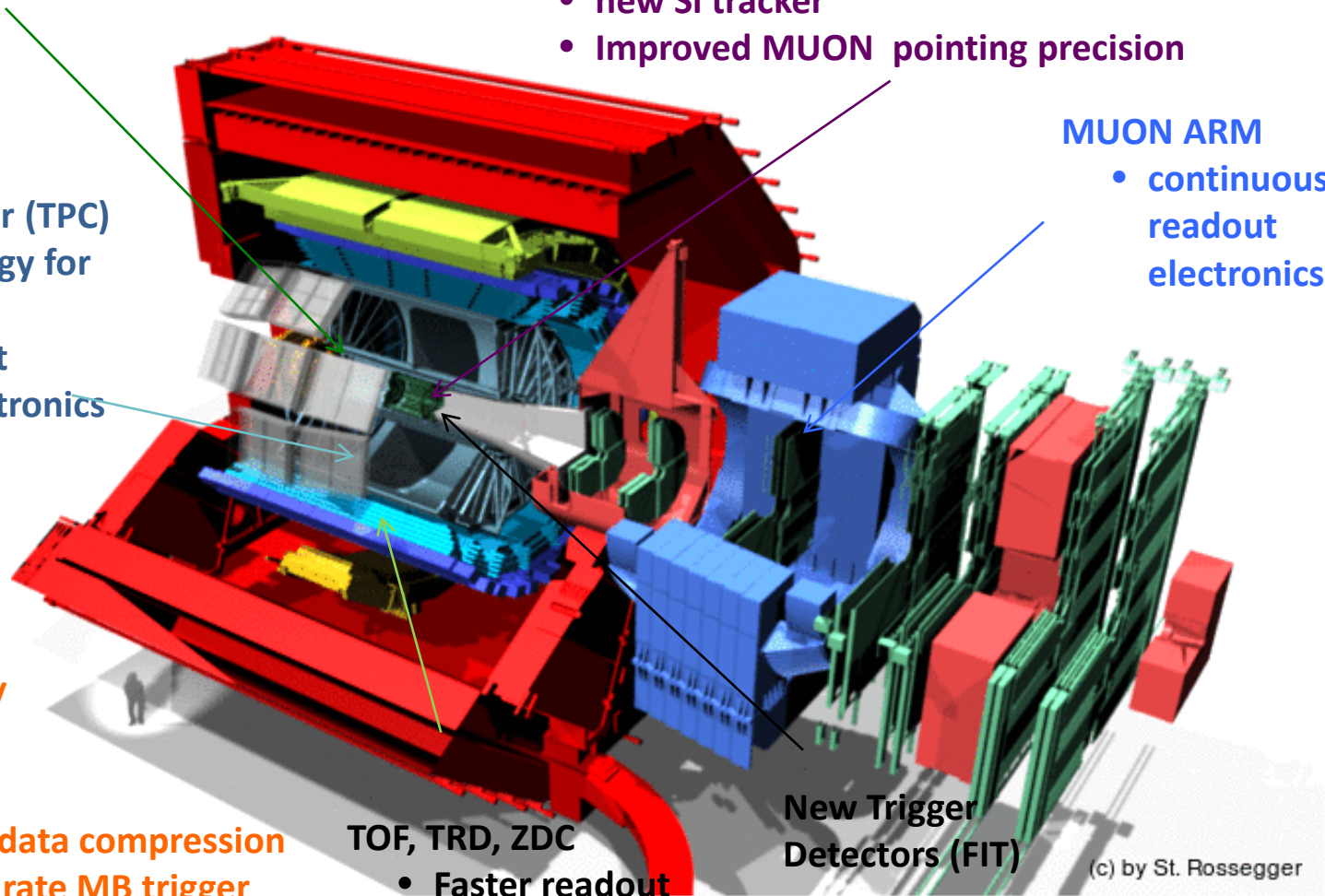
Data Acquisition (DAQ)/ High Level Trigger (HLT)

- new architecture
- on line tracking & data compression
- 50kHz PbPb event rate MB trigger

TOF, TRD, ZDC

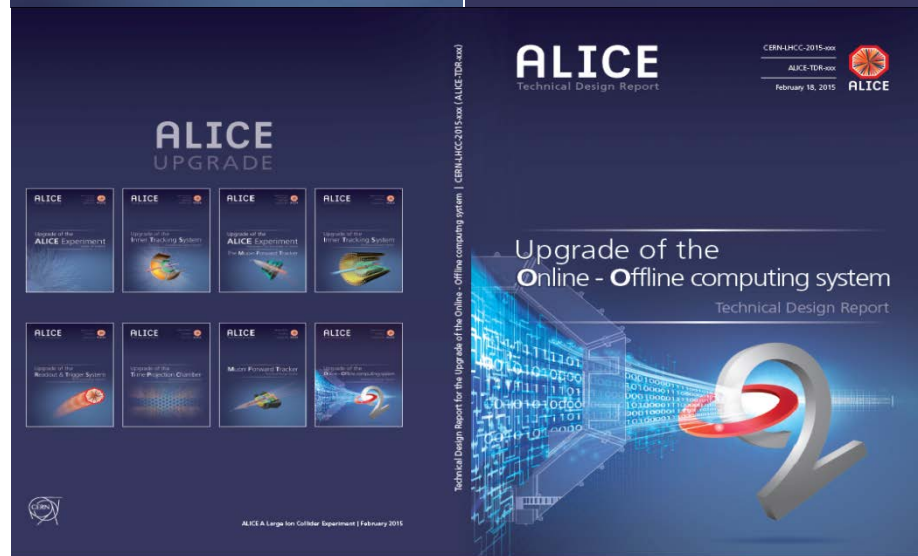
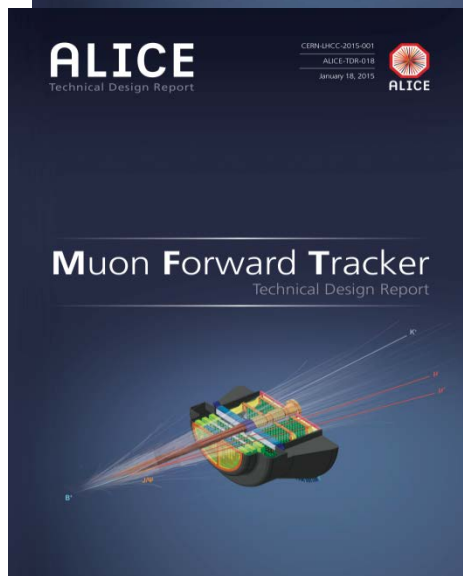
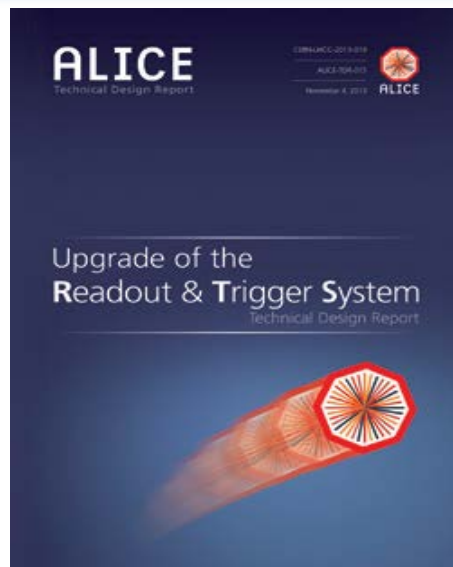
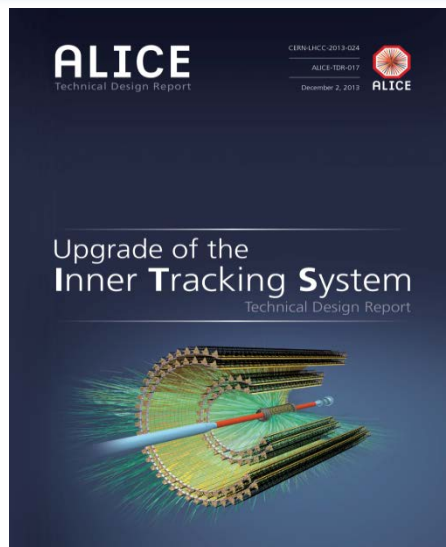
- Faster readout

New Trigger Detectors (FIT)

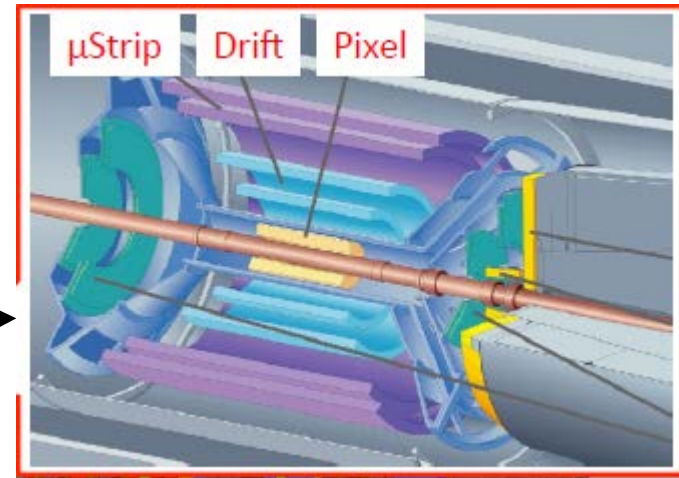
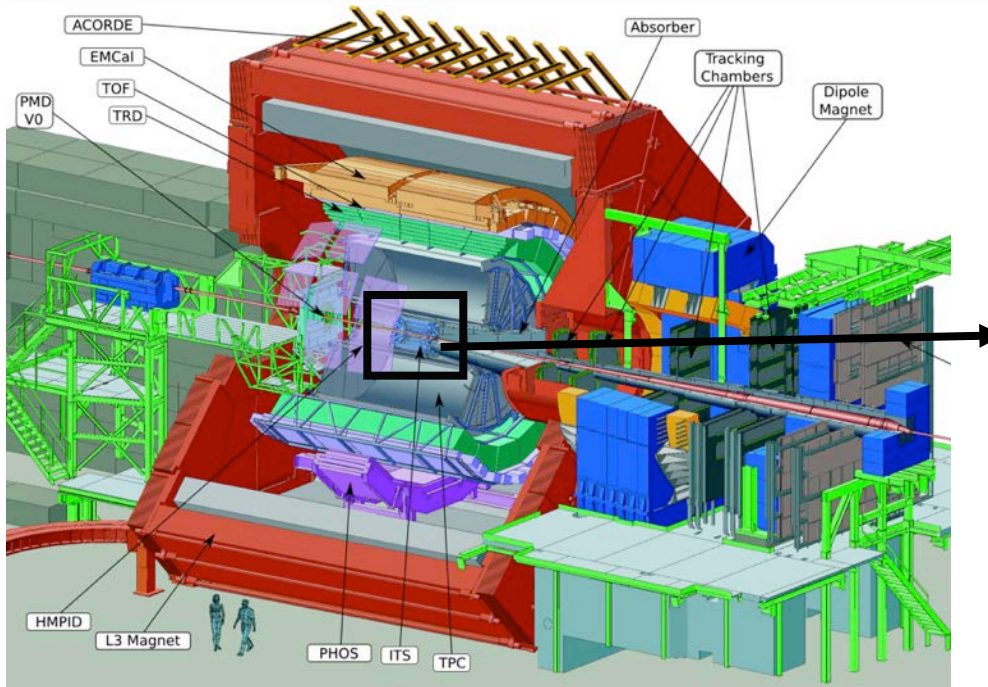


(c) by St. Rossegger

Major upgrade program for run 3



ALICE new ITS



$r_{in} = 3.9$ cm (beam pipe wall)
 $r_{out} = 43$ cm (track matching with TPC)

•7- layer barrel geometry of MAPS (Monolithic Active Pixel Sensors)

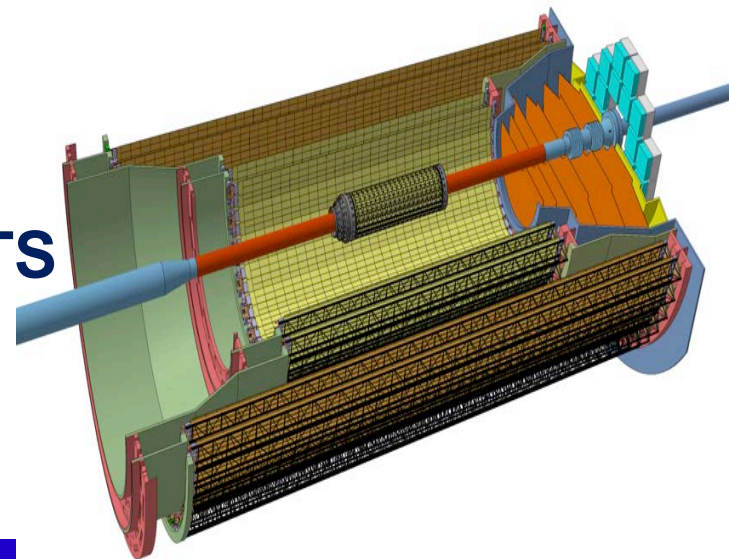
- Inner Barrel → 3 layers , $z=29$ cm
- Outer Barrel → 4 layers, $z=90, 150$ cm

New ITS

•25 G pixels, $\sim 10\text{m}^2$

•Pseudorapidity coverage: $|\eta| \leq 1.2$

•r coverage: 2.2 – 43 cm



ITS Upgrade Features

1. Improve impact parameter resolution by a factor 3

- Get closer to IP (position of first layer): **39 mm** → **23 mm**
- Reduce x/X_0 /layer : **~1.14%** → **~ 0.3%** (for inner layers) **~ 0.8%** (for outer layers)
- Reduce pixel size: $50\mu\text{m} \times 425\mu\text{m}$ → $O(30\mu\text{m} \times 30\mu\text{m})$

2. Improve tracking efficiency and p_T resolution at low p_T .

- Increase granularity:
6 layers → **7 layers**
silicon drift and strips → **pixels**

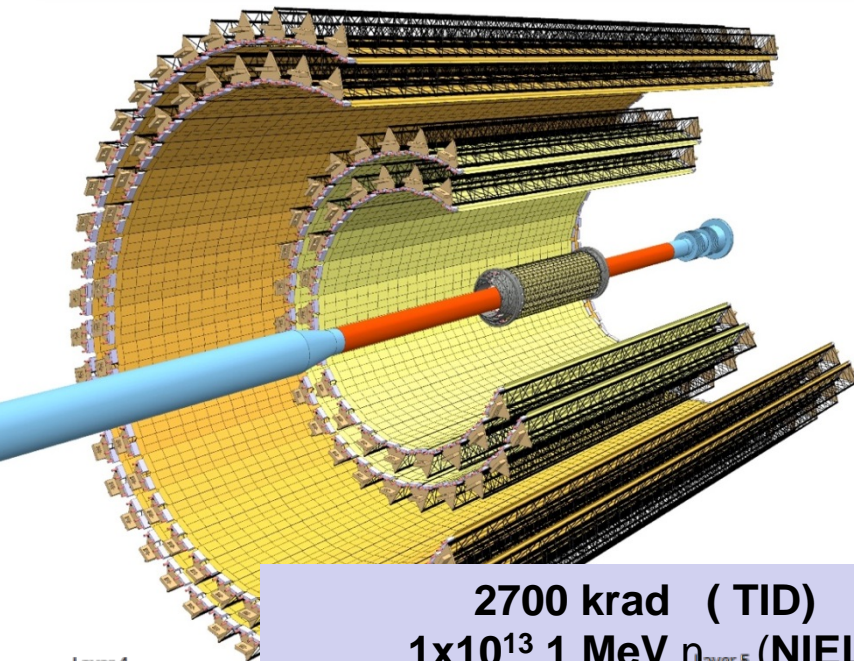
3. Fast readout.

- Readout Pb-Pb interactions at **>100 kHz** and pp interactions at **~several 10^5 Hz**.
- (currently limited at **1kHz** with full ITS)

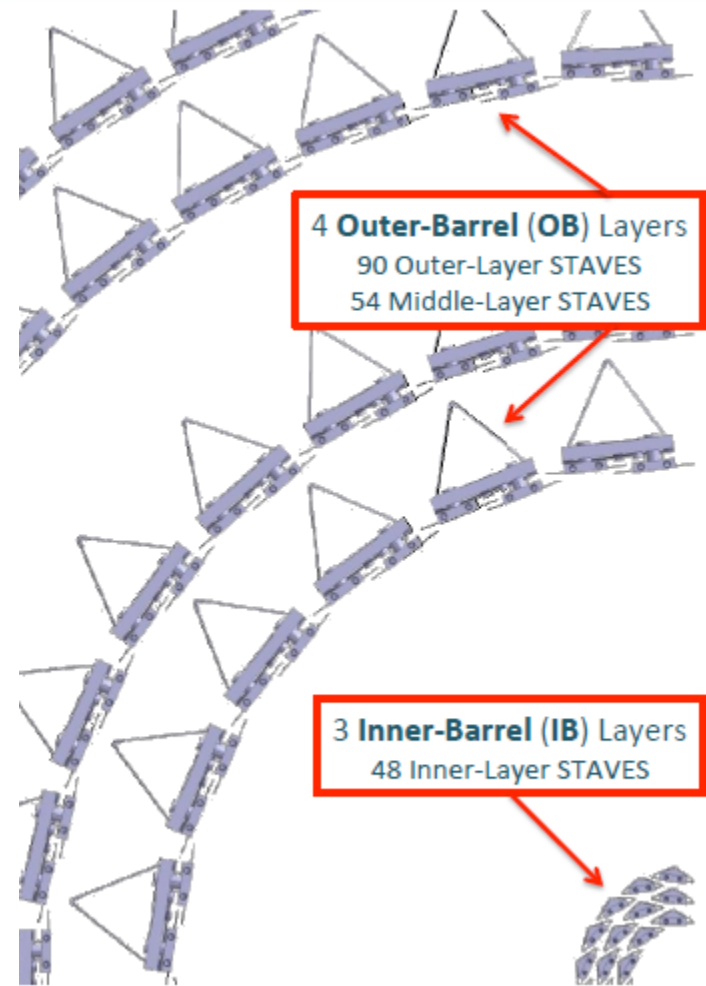
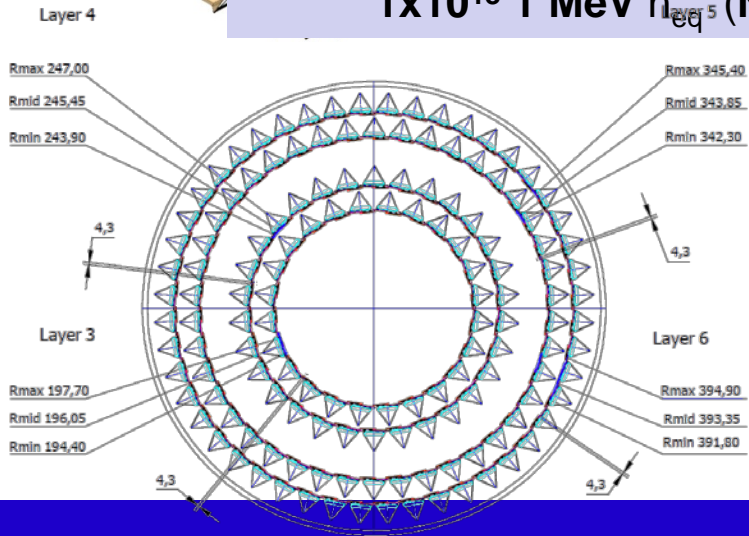
4. Fast insertion/removal for yearly maintenance

- Possibility to replace non functioning detector modules during yearly shutdown.

ALICE new ITS Layout



2700 krad (TID)
 1×10^{13} 1 MeV n_{eq} (NIEL)

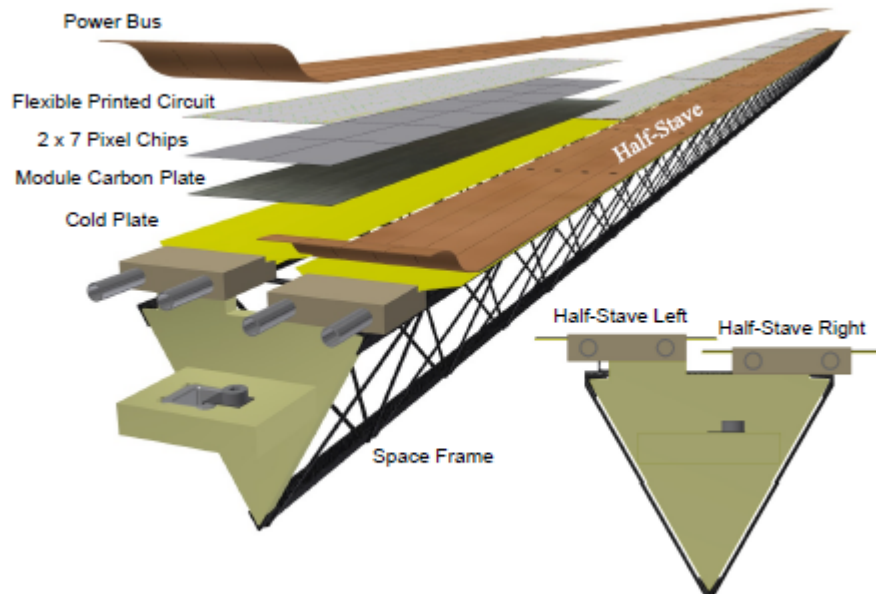


4 Outer-Barrel (OB) Layers
 90 Outer-Layer STAVES
 54 Middle-Layer STAVES

3 Inner-Barrel (IB) Layers
 48 Inner-Layer STAVES

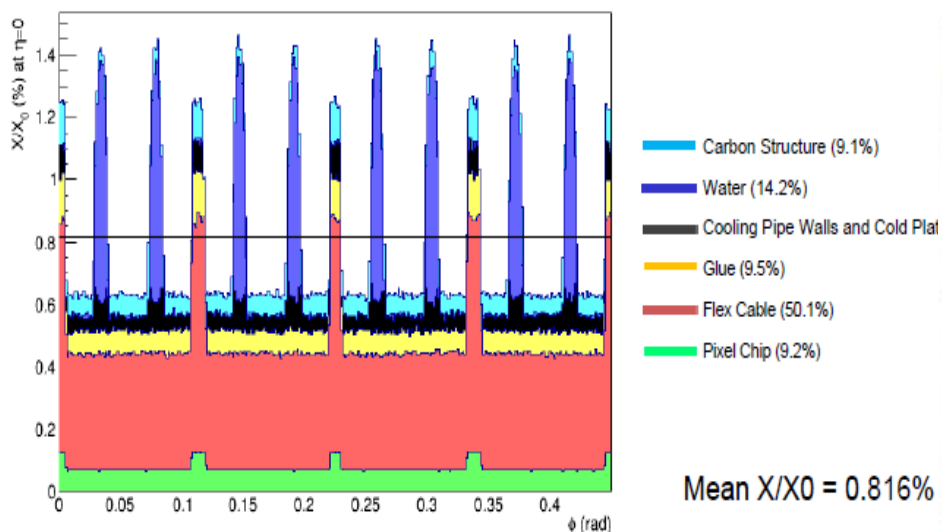
Layers are azimuthally segmented in STAVES
Staves have independent mechanics, power, cooling and readout.

ALICE new ITS: outer layers

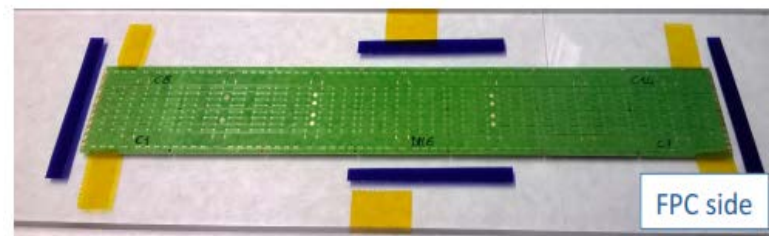


Length 150 cm Weight 30 gr

Module = Hybrid Integrated Circuit (HIC)
Flexible Printed Circuit + 14 pixel chips



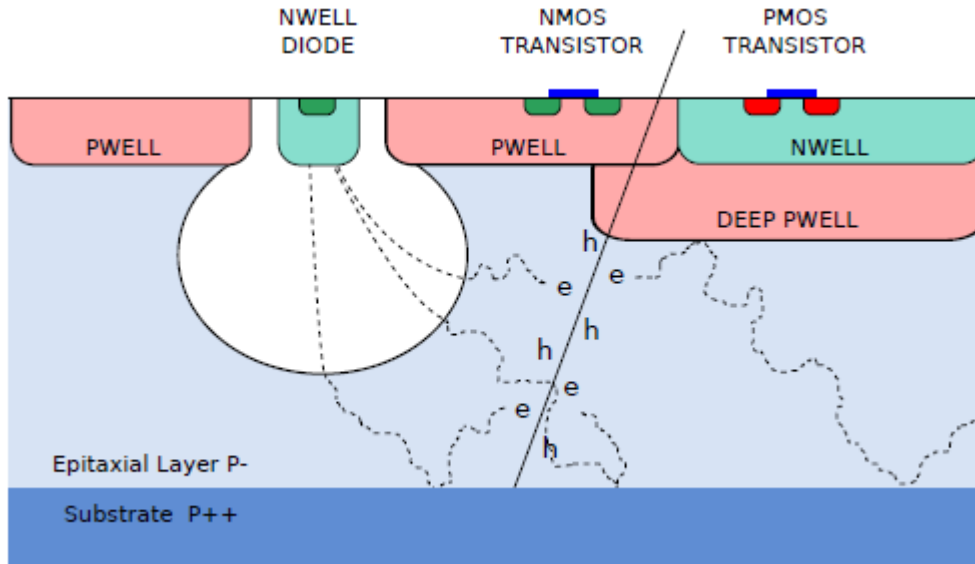
sensor side



FPC side

Pixel chip technology

Monolithic Active Pixel Sensors using TowerJazz 0.18 μm CMOS Imaging Process



- High resistivity ($> 1\text{k}\Omega\text{cm}$) p-type epitaxial layer (20-40 μm thick) on substrate.
- Small n-well diode (2-3 μm diameter) ~much smaller than the depletion zone.
- Application of moderate reverse bias voltage to substrate depletes the depletion zone around NWELL collection diode.
- Deep pWELL shields NWELL of PMOS transistor, allowing for full CMOS circuitry within active area.

Feature
Gate
Metal

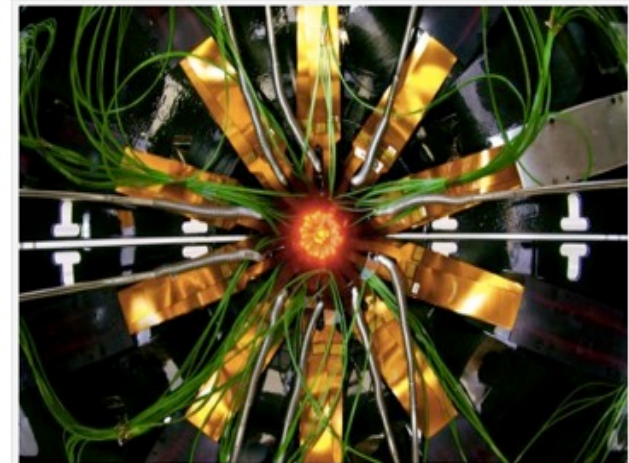
TechTime Electronics & Technology News

News | Business | Technology | Hebrew

TowerJazz will develop CERN's Image Sensor

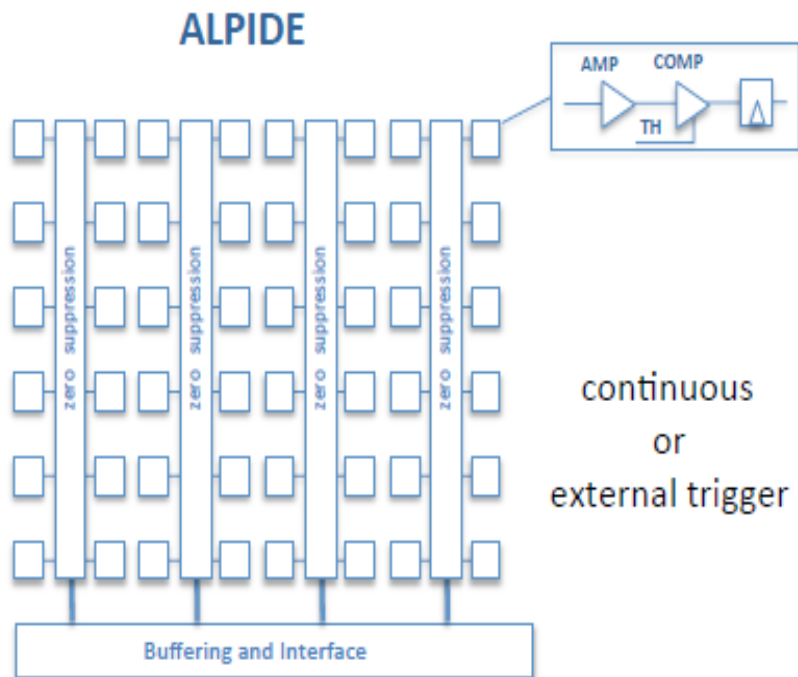
Published 22 November 2013

The global specialty foundry TowerJazz, said it was chosen to provide the sensor for the upgrade of the Inner Tracking System (ITS) of the ALICE experiment at the European Organisation for Nuclear Research (CERN) in Geneva, Switzerland.



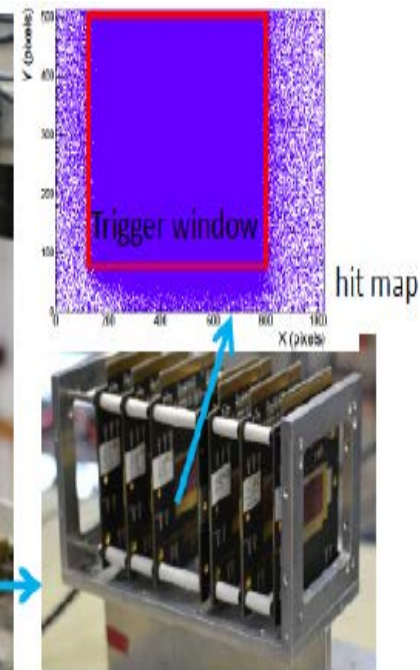
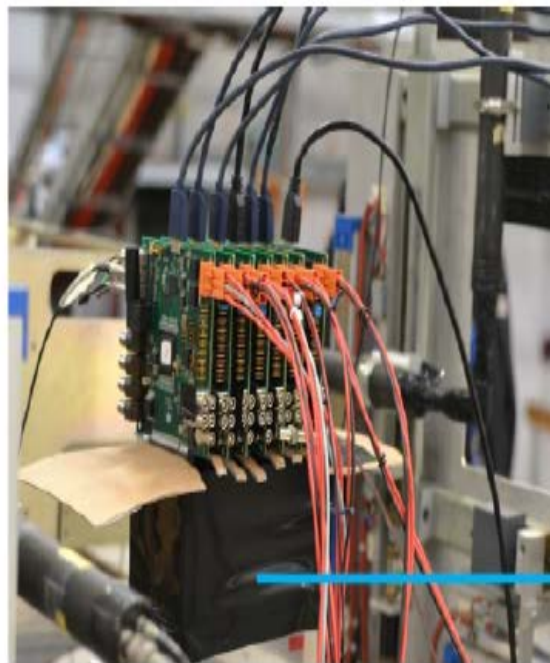
ALICE detector on the Large Hadron Collider ring in CERN

Pixel Chip Features, Architecture and Characterization

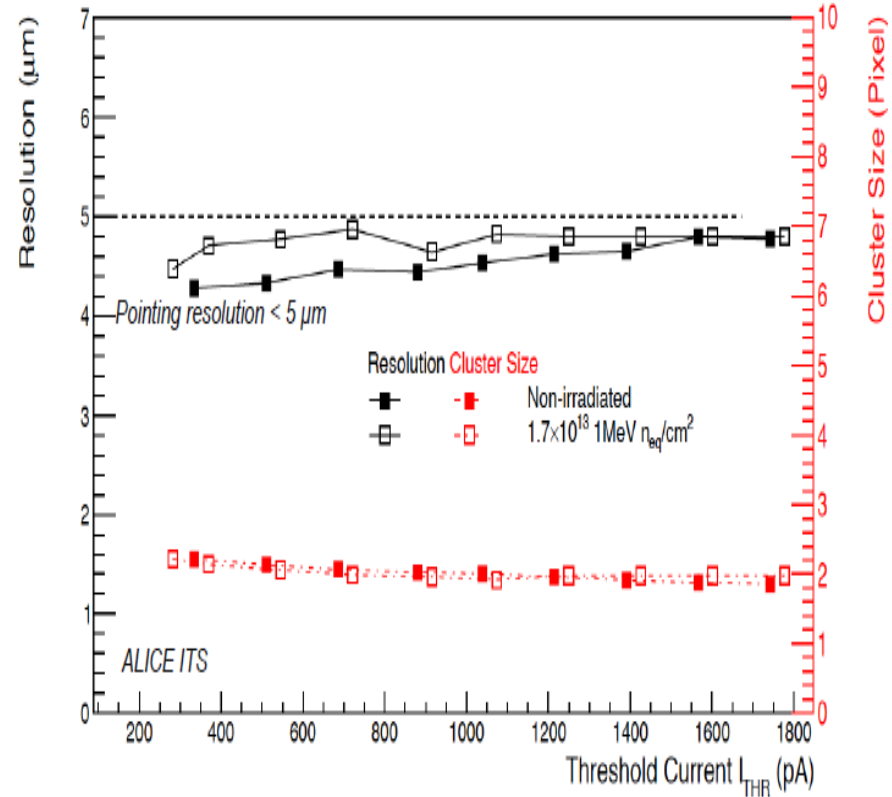
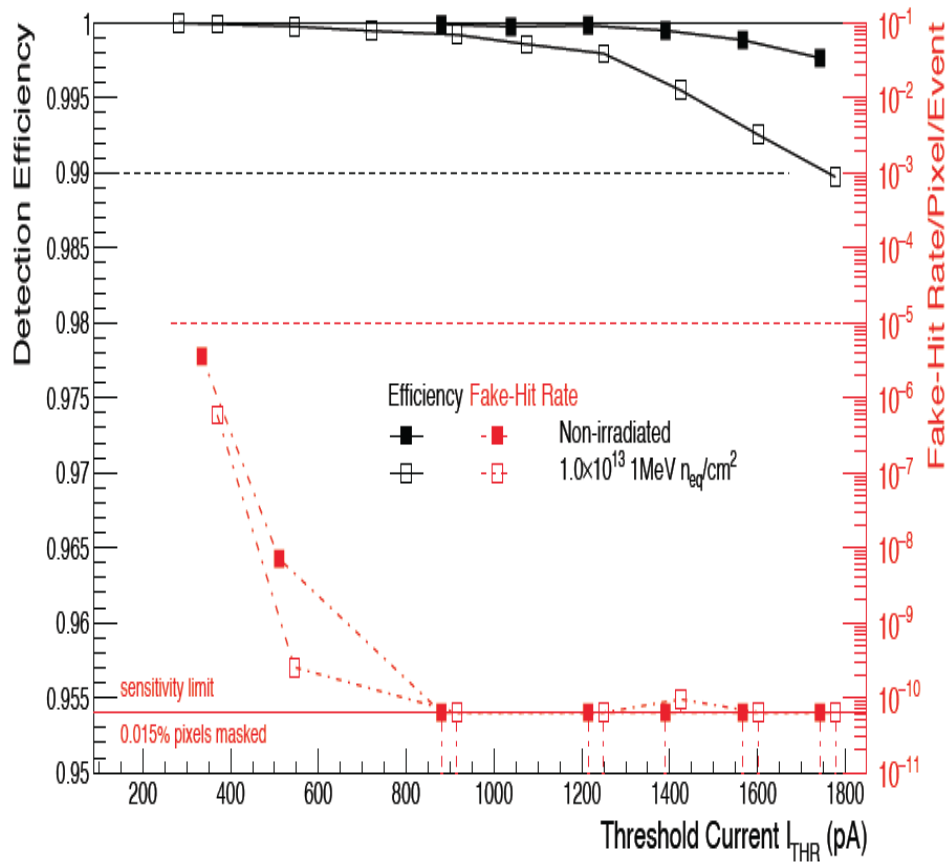


- PS: 5-7 GeV π^+
- SPS: 120 GeV π^+
- PAL (Korea): 60 MeV e^-
- BTF (Frascati): 450 MeV e^-
- DESY: 5.8 GeV e^+

Pixel pitch	28 μ m x 28 μ m
Event time resolution	<2 μ s
Power consumption	39mW/cm ²
Dead area	1.1 mm x 30mm



Efficiency and Resolution



3 chips not irradiated and 3 chips irradiated neutrons 10^{13} 1MeV n_{eq}/cm^2

λ fake $\ll 10^{-5}$ event/pixel and $\epsilon_{det} > 99.5\%$

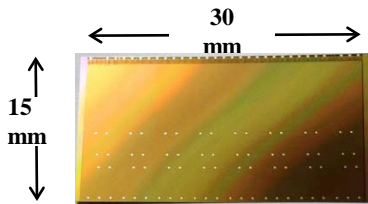
Resolution $\leq 5 \mu m$

HIC assembly and interconnections

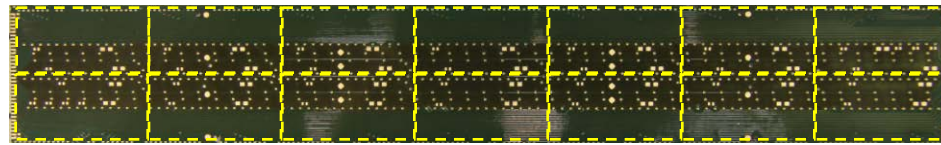
Pixel chip 100 μ m thick
with pads over logic

Flexible Printed Circuit (FPC):
double layer Cu/Polyimide

Cross-cables for
connection to Power Bus



x 14



x 1



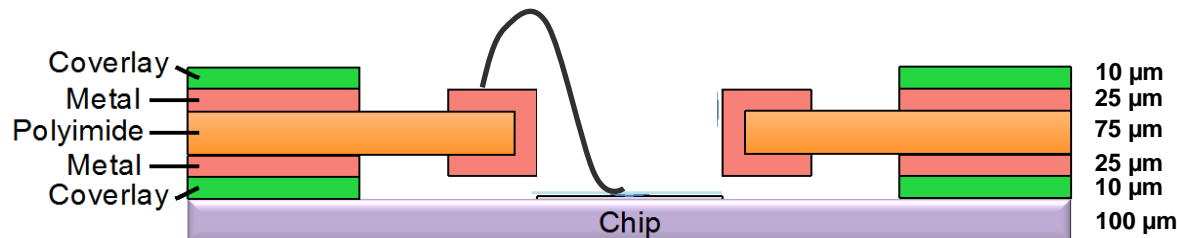
x 6 (4xVDD + 2xGND)

Chip-to-FPC mechanical connection

Gluing with non conductive, two components, epoxy adhesive

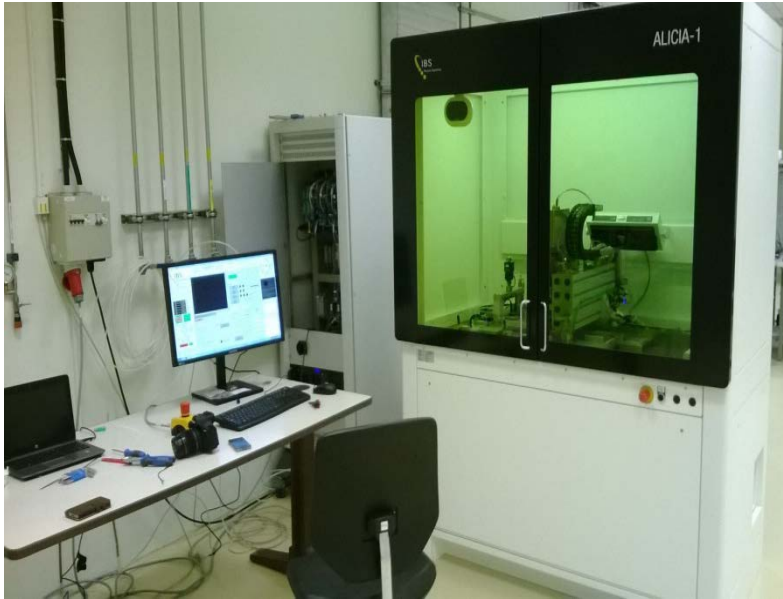
Flip-chip bonding

Wire-bonding through the vias in the FPC (~1000 connection/HIC)



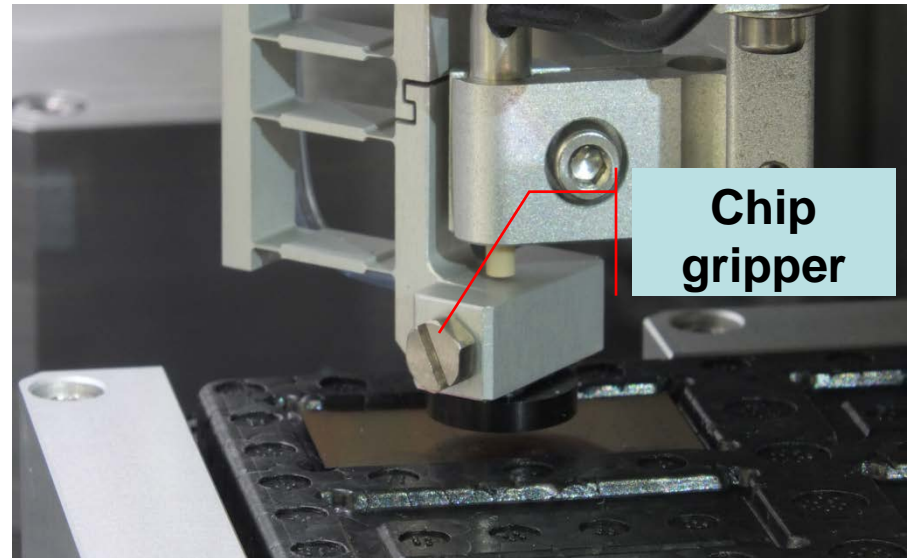
HIC assembly stack-up

HIC Assembly @ Bari

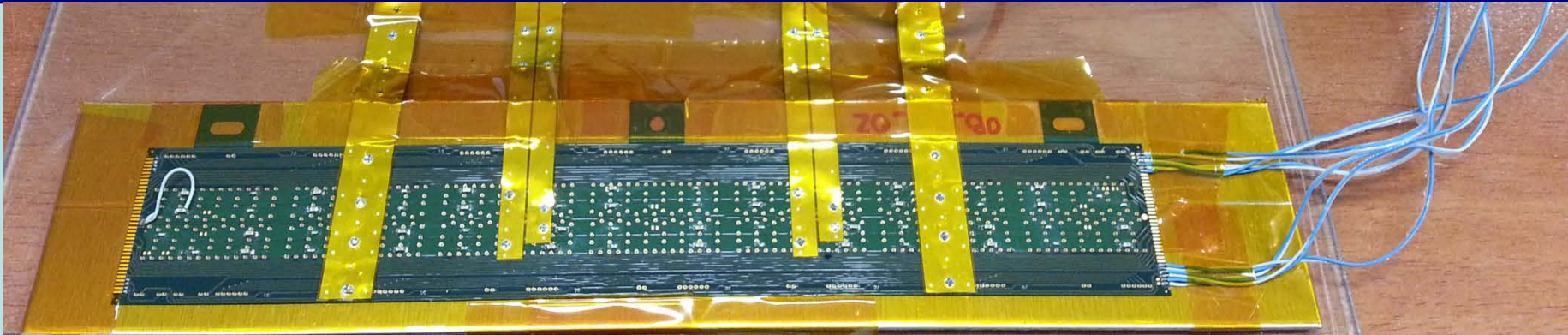


The machine will perform:

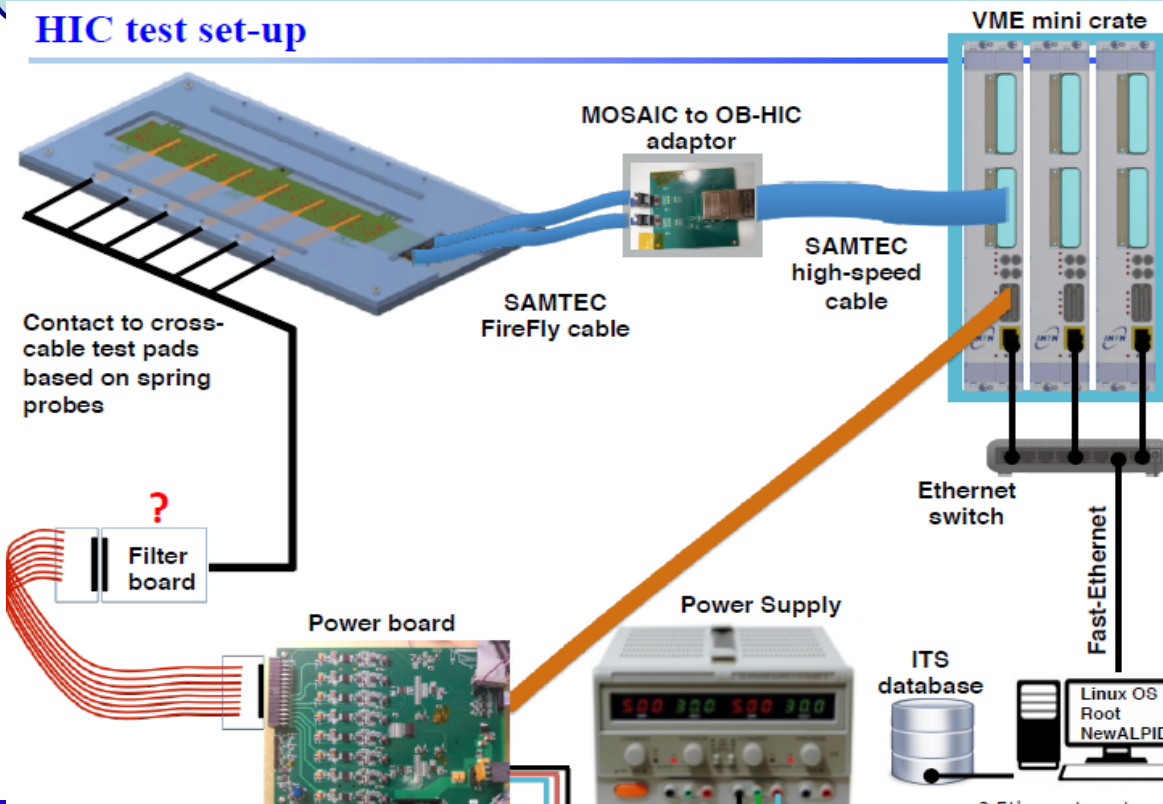
- placement of chips with $\pm 5 \mu\text{m}$ accuracy wrt external markers
- Automatic Optical Inspection: chips dimensions, chip edge integrity, chip interconnection pads cleanliness, chip positions in HIC



HIC characterization



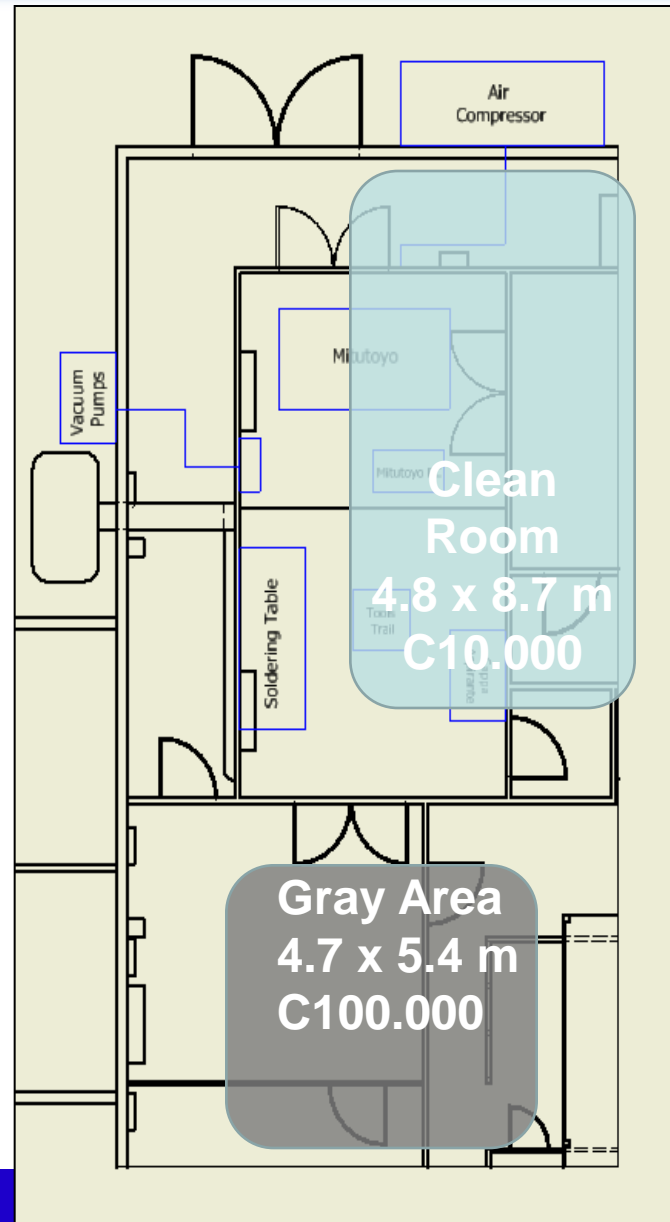
HIC test set-up



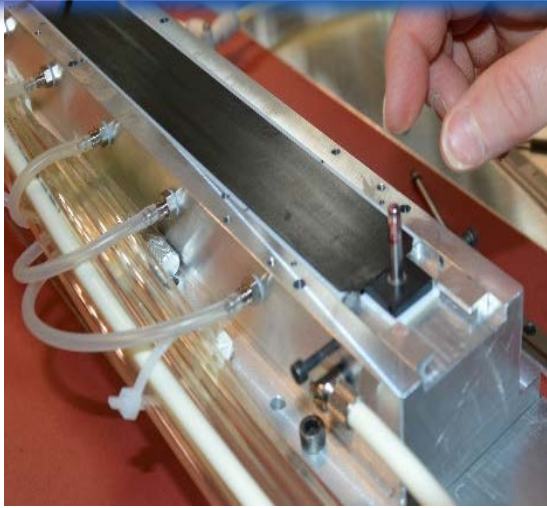
HIC OB 16	# good pixels	# dead pixels	Mean Threshold	< Noise >
CHIP 0	524275	13	125.43	4.73
CHIP 1	522241	2047	155.93	5.54
CHIP 2	524284	4	129.83	5.07
CHIP 3	523263	1025	130.98	4.89
CHIP 4	524286	2	158.26	5.45
CHIP 5	523508	780	134.44	5.10
CHIP 6	524116	172	164.22	5.88
CHIP 8	523262	1026	158.69	5.72
CHIP 9	524283	5	145.17	5.62
CHIP 10	523259	1029	158.75	5.88
CHIP 11	523263	1025	131.46	5.31
CHIP 12	523711	577	135.11	5.14
CHIP 13	524282	6	127.07	4.76
CHIP 14	524285	3	132.77	4.93

LNf infrastructure for Stave Assembly

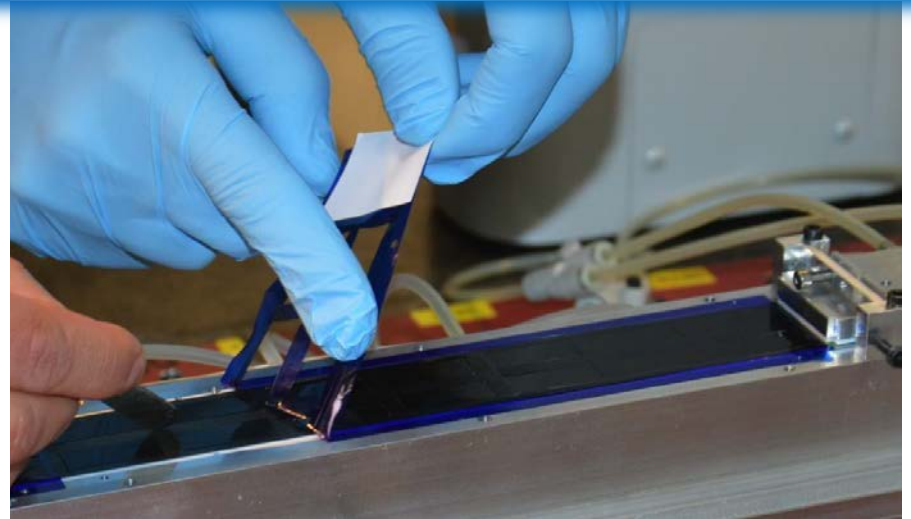
- Mitutoyo Crysta Apex S 9206
- Final jig installed and ready
- Grey area for:
HIC test
Stave operations
(PB soldering and tests)



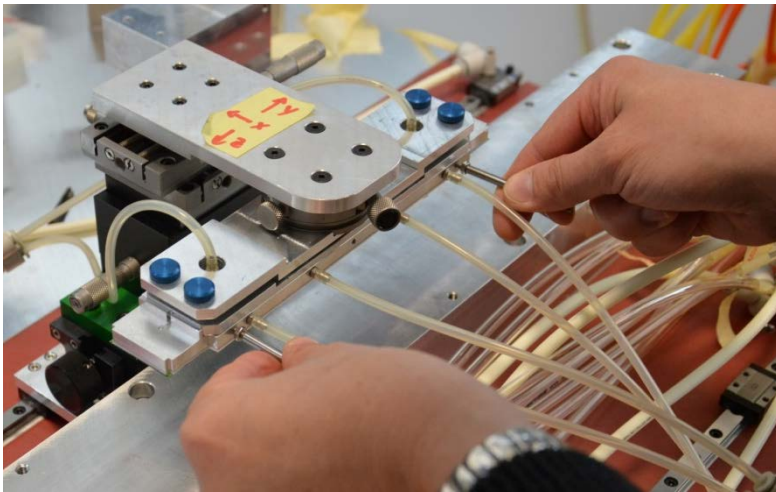
Half Stave assembly steps (1)



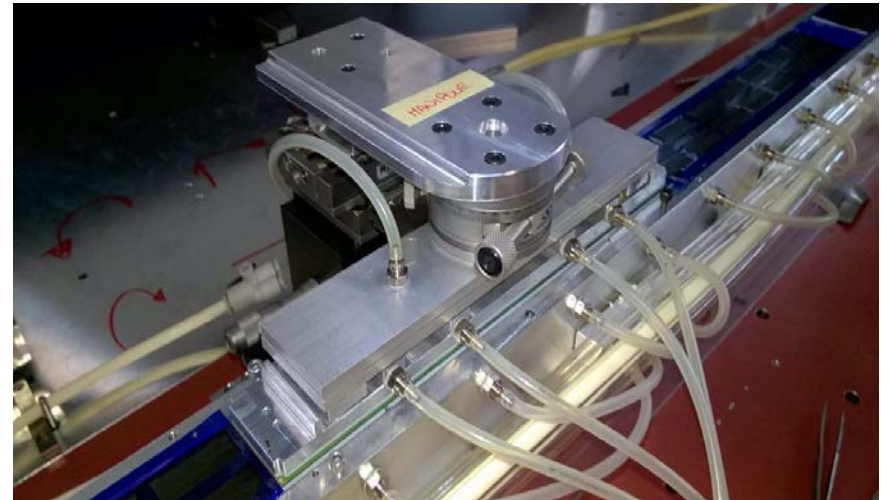
1) cold plate alignment



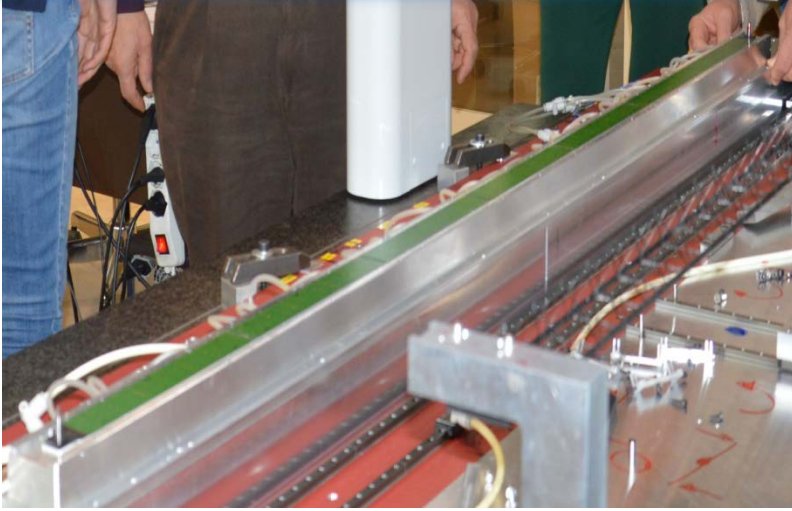
2) glue deposition



3) HIC module alignment (10 μm precision)



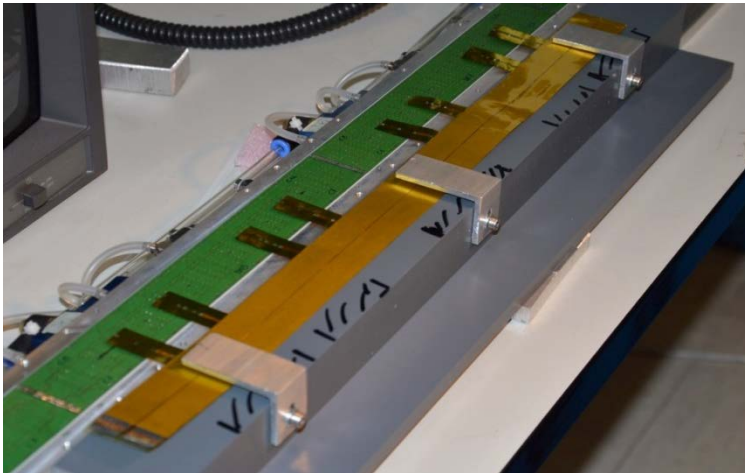
Half Stave assembly steps (2)



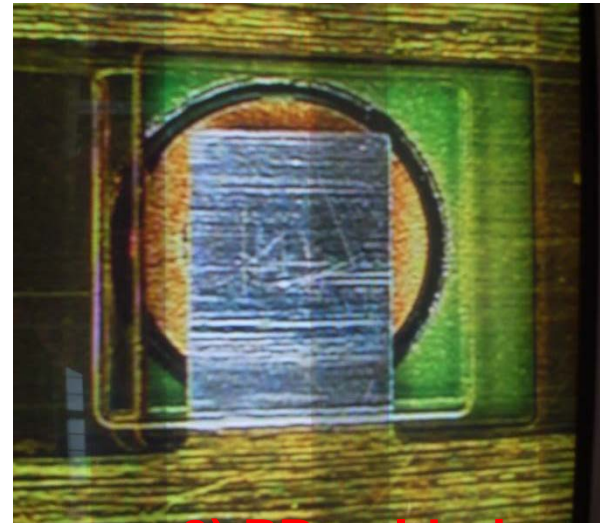
5) modules x7 aligned and glued



6) HIC to HIC connections

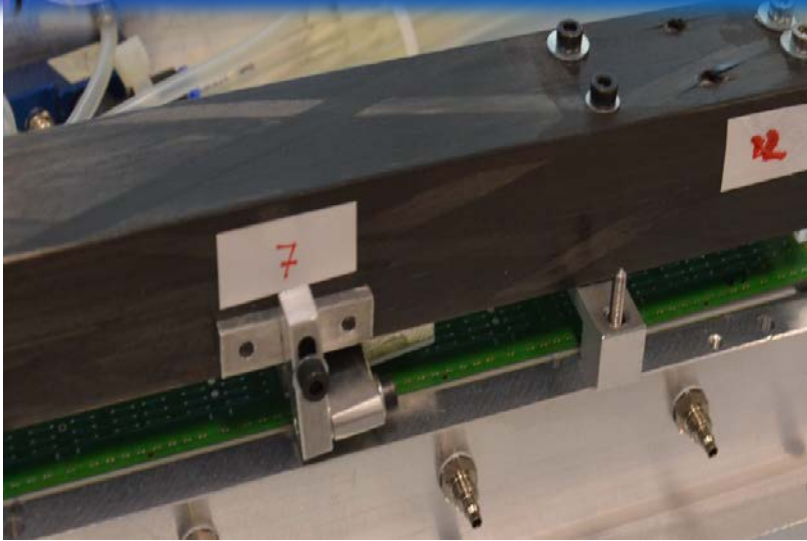


7) PB alignment



8) PB soldering

Half Stave assembly steps (3)



9) Handling bar placed on the HS



10) HS rotated and placed on the alignment station



11) HS aligned and placed under SF



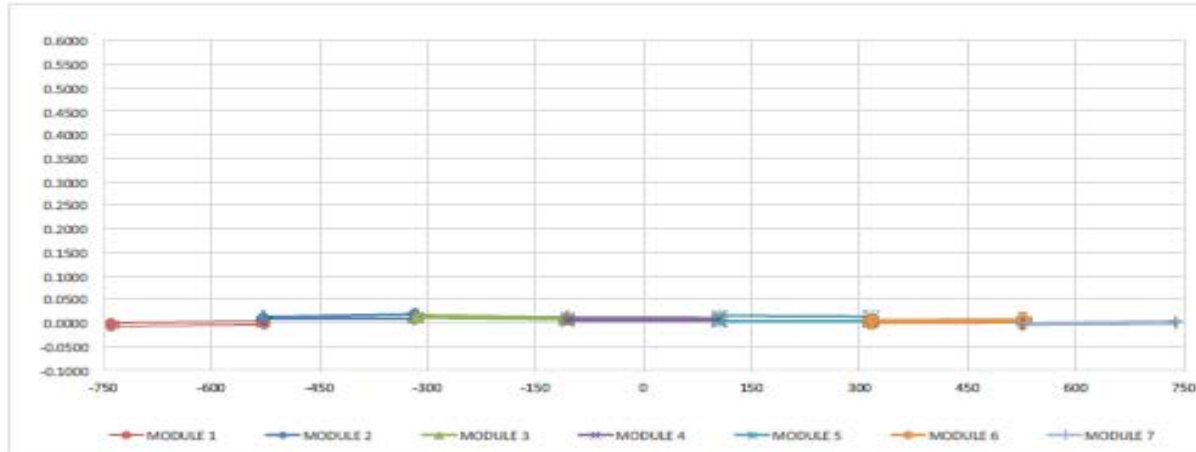
12) HS glued to SF

Half Stave 0

HICEL

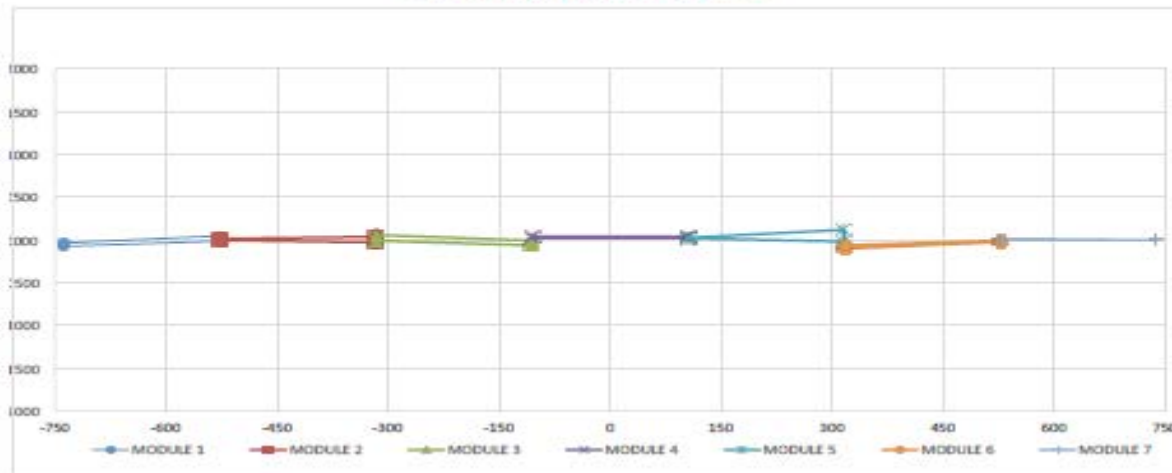
For each HIC the position of reference marker on the 4 corners was measured after each HS assembly
We report the deviations from the nominal position along Y coordinate.

Precise positioning along this coordinate depends on the precision of the TAB cut: TAB were all cut at 80-100 μ m from the sensor



Max Deviation [mm] = 0.0167
RMS [mm]=0.006

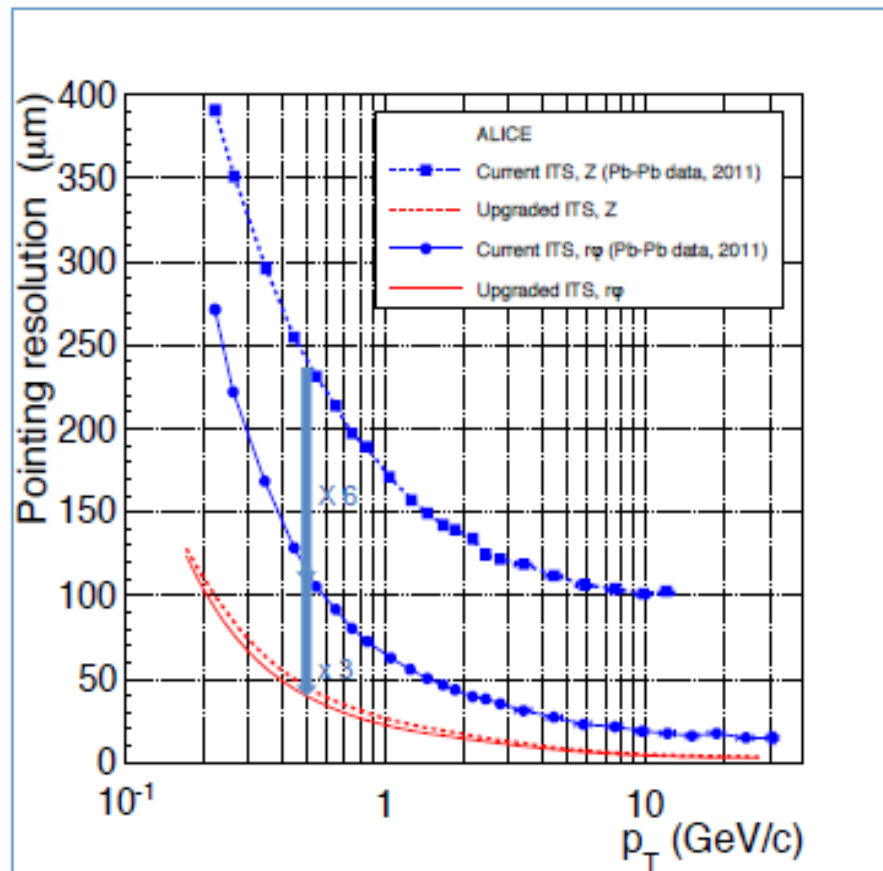
ΔX FROM NOMINAL VALUE [mm]



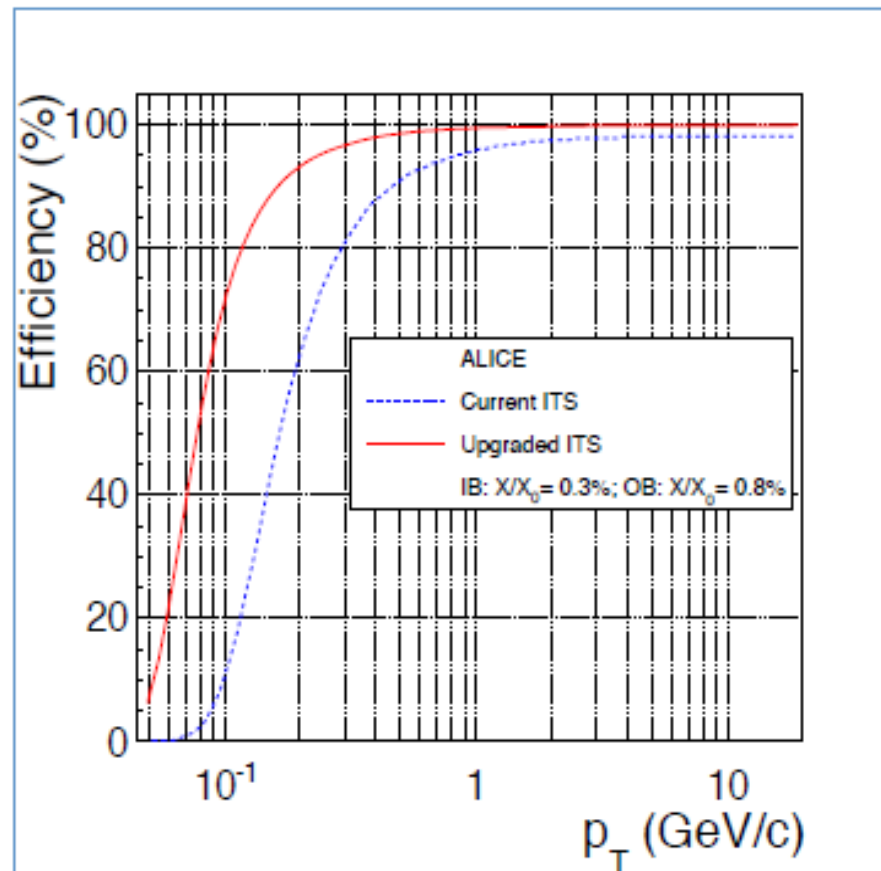
Max Deviation [mm] = 0.011
RMS [mm]=0.004

Performance of the new ITS

Impact parameter resolution



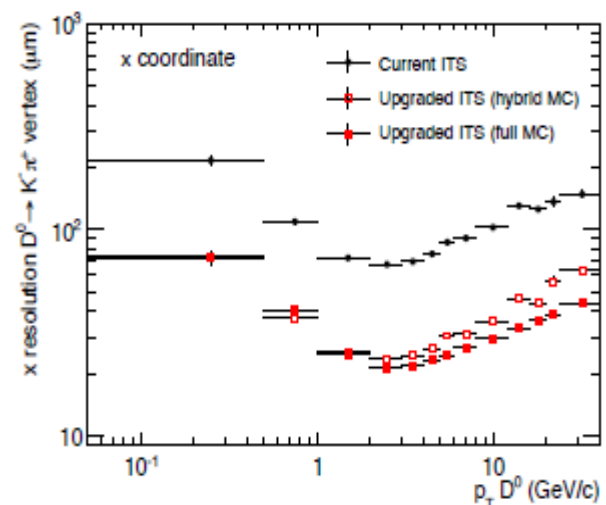
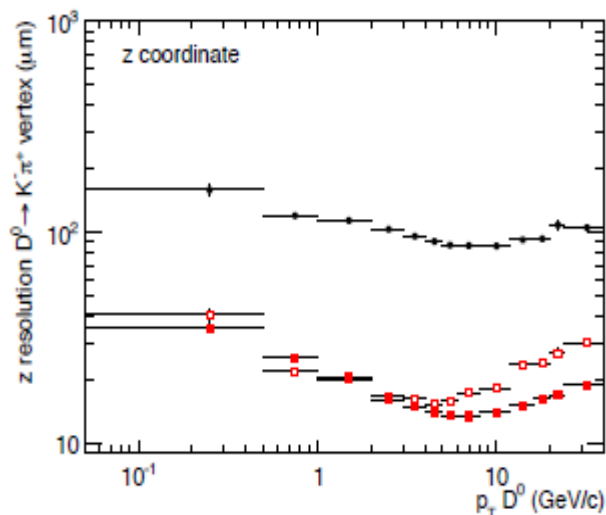
Tracking efficiency (ITS standalone)



$\sim 40 \mu\text{m}$ at $p_T = 500 \text{ MeV}/c$

Physics Performance of the new ITS

Esempio: $D^0 \rightarrow K\pi^+$



Altri canali notevoli

Observable	Current, 0.1 nb^{-1}		Upgrade, 10 nb^{-1}	
	p_T^{min} (GeV/c)	statistical uncertainty	p_T^{min} (GeV/c)	statistical uncertainty
Heavy Flavour				
D meson R_{AA}	1	10 %	0	0.3 %
D_s meson R_{AA}	4	15 %	< 2	3 %
D meson from B R_{AA}	3	30 %	2	1 %
J/ψ from B R_{AA}	1.5	15 % ($p_T\text{-int.}$)	1	5 %
B^+ yield	not accessible		3	10 %
Λ_c R_{AA}	not accessible		2	15 %
Λ_c/D^0 ratio	not accessible		2	15 %
Λ_b yield	not accessible		7	20 %
D meson v_2 ($v_2 = 0.2$)	1	10 %	0	0.2 %
D_s meson v_2 ($v_2 = 0.2$)	not accessible		< 2	8 %
D from B v_2 ($v_2 = 0.05$)	not accessible		2	8 %
J/ψ from B v_2 ($v_2 = 0.05$)	not accessible		1	60 %
Λ_c v_2 ($v_2 = 0.15$)	not accessible		3	20 %
Dielectrons				
Temperature (intermediate mass)	not accessible			10 %
Elliptic flow ($v_2 = 0.1$)	not accessible			10 %
Low-mass spectral function	not accessible		0.3	20 %
Hypernuclei				
$^3_\Lambda\text{H}$ yield	2	18 %	2	1.7 %

Outer Barrel ITS

Sezione/Laboratorio	Principali Responsabilità
Bari	<ul style="list-style-type: none">• Modulo OB: Procedura Assemblaggio, Modulo 0, Produzione• Sistema di Test per Moduli e Stave• Power Supply System
Cagliari	<ul style="list-style-type: none">• Architettura del chip (Priority encoder & R/O Interface)• Sistema di test per Pixel Chip
Catania	<ul style="list-style-type: none">• Test Elettrici degli FPC per l'OB (in collaborazione con Trieste)
LNF+Roma	<ul style="list-style-type: none">• Produzione Stave OB• LNF Beam Test Facility
Padova	<ul style="list-style-type: none">• Integrazione OB: End-wheels, Conical Structural Shell, Integrazione Half-Layer e Half-barrel
Torino+Alessandria	<ul style="list-style-type: none">• PLL & DTU del Pixel Chip• Progettazione del FPC• Stave OB: Procedura di Assemblaggio, Stave 0, Produzione
Trieste	<ul style="list-style-type: none">• Produzione e test degli FPC per gli OB

Conclusions

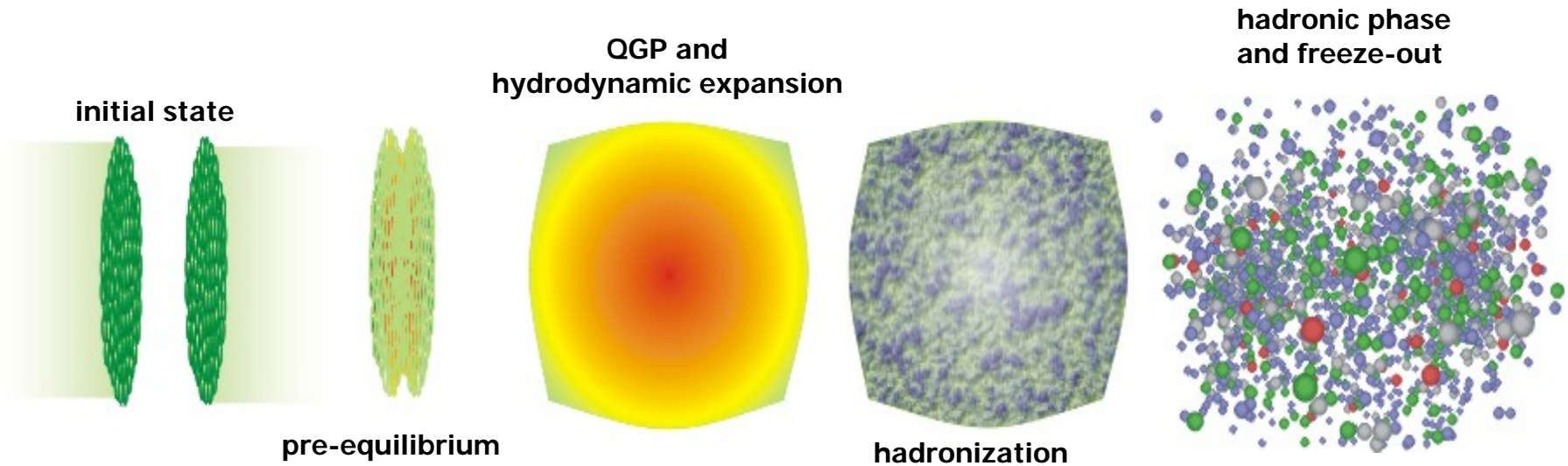
ALICE sta producendo risultati interessanti ed “intriganti” che stanno emergendo dalle analisi sui dati dei Run I e II (attualmente in corso).

Sono in costruzione una serie di Upgrades del rivelatore, tra cui il nuovo ITS che vede fortemente coinvolti i gruppi italiani, che entreranno in operazione per il RUNIII.

Abbiamo bisogno di tutto il supporto possibile da parte dei gruppi teorici per l'interpretazione/modellizzazione dei nuovi risultati e per quelli che dovranno arrivare....

**Anche la costruzione dei gli upgrades richiede un notevole impegno...
Chiunque interessato in questa 'impresa' e' ovviamente il benvenuto!**

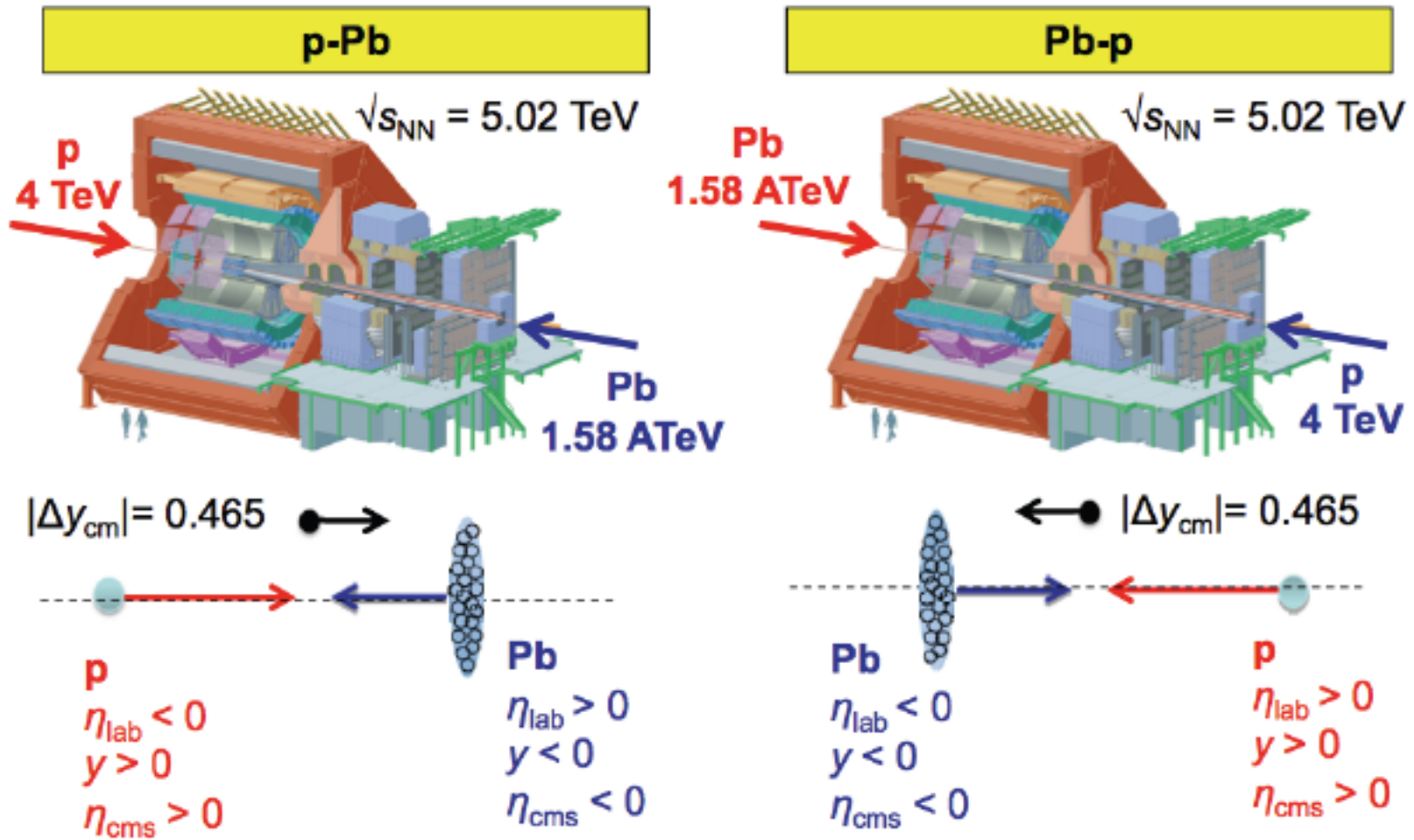
High Energy Nucleus-Nucleus Collisions



Physics:

- 1) Parton distributions in nuclei
- 2) Initial conditions of the collision
- 3) a new state of matter – Quark-Gluon Plasma and its properties
- 4) hadronization

p-Pb collision geometry

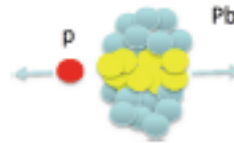


the direction for the proton is always at positive $y \equiv y_{cms}$ and positive η_{cms}

Centrality — Introduction



- In contrast to Pb-Pb collisions, it is not straightforward to relate experimental quantities to the collision geometry, i.e. the number of participants N_{part} and binary collisions N_{coll} .
→ in p-Pb collisions: $N_{coll} = N_{part} - 1$



- Large biases present in the system:
 - Multiplicity fluctuations
 - Jet-veto bias
 - Geometric bias

- Most simple approach: only multiplicity classes instead of centrality, but more can be done...

